



waste

Article

Optimization of Biomass Delignification by Extrusion and Analysis of Extrudate Characteristics

Delon Konan, Adama Ndao, Ekoun Koffi, Saïd Elkoun, Mathieu Robert, Denis Rodrigue and Kokou Adjallé



<https://doi.org/10.3390/waste3020012>

Article

Optimization of Biomass Delignification by Extrusion and Analysis of Extrudate Characteristics

Delon Konan ¹, Adama Ndao ¹, Ekoun Koffi ², Saïd Elkoun ³, Mathieu Robert ³, Denis Rodrigue ⁴ and Kokou Adjallé ^{1,*}

- ¹ Laboratory of Environmental Biotechnologies, Institut National de la Recherche Scientifique (INRS), Quebec City, QC G1P 4S5, Canada; behibro_ange-delon.konan@inrs.ca (D.K.); adama.ndao@inrs.ca (A.N.)
- ² Department of Mechanic and Energy Engineering, Institut National Polytechnique Felix Houphouët Boigny (INPHB), Yamoussoukro BP 1093, Côte d'Ivoire; ekoun.koffi@inphb.ci
- ³ Center for Innovation in Technological Ecodesign (CITE), University of Sherbrooke, Sherbrooke, QC J1K 2R1, Canada; said.elkoun@usherbrooke.ca (S.E.); mathieu.robert2@usherbrooke.ca (M.R.)
- ⁴ Department of Chemical Engineering, Université Laval, Quebec City, QC G1V 0A6, Canada; denis.rodrigue@gch.ulaval.ca
- * Correspondence: kokou.adjalle@inrs.ca

Abstract: Pretreatment of lignocellulosic biomass remains the primary obstacle to the profitable use of this type of biomass in biorefineries. The challenge lies in the recalcitrance of the lignin-carbohydrate complex to pretreatment, especially the difficulty in removing the lignin to access the carbohydrates (cellulose and hemicellulose). This study had two objectives: (i) to investigate the effect of reactive extrusion on lignocellulosic biomass in terms of delignification percentage and the structural characteristics of the resulting extrudates, and (ii) to propose a novel pretreatment approach involving extrusion technology based on the results of the first objective. Two types of biomasses were used: agricultural residue (corn stover) and forest residue (black spruce chips). By optimizing the extrusion conditions via response surface analysis (RSA), the delignification percentages were significantly improved. For corn stover, the delignification yield increased from 2.3% to 27.4%, while increasing from 1% to 25.3% for black spruce chips. The highest percentages were achieved without the use of sodium hydroxide and for temperatures below 65 °C. Furthermore, the optimized extrudates exhibited important structural changes without any formation of p-cresol, furfural, and 5-hydroxymethylfurfural (HMF) (enzymes and microbial growth-inhibiting compounds). Acetic acid however was detected in corn stover extrudate. The structural changes included the disorganization of the most recalcitrant functional groups, reduction of particle sizes, increase of specific surface areas, and the appearance of microscopic roughness on the particles. Analyzing all the data led to propose a new promising approach to the pretreatment of lignocellulosic biomasses. This approach involves combining extrusion and biodelignification with white rot fungi to improve the enzymatic hydrolysis of carbohydrates.

Keywords: biomass pretreatment; extrusion; pretreatment optimization; response surface methodology; biodelignification



Academic Editor: Gassan Hodaifa

Received: 27 January 2025

Revised: 14 March 2025

Accepted: 20 March 2025

Published: 25 March 2025

Citation: Konan, D.; Ndao, A.; Koffi, E.; Elkoun, S.; Robert, M.; Rodrigue, D.; Adjallé, K. Optimization of Biomass Delignification by Extrusion and Analysis of Extrudate Characteristics. *Waste* **2025**, *3*, 12. <https://doi.org/10.3390/waste3020012>

Copyright: © 2025 by the authors.

Licensee MDPI, Basel, Switzerland.

This article is an open access article distributed under the terms and conditions of the Creative Commons Attribution (CC BY) license (<https://creativecommons.org/licenses/by/4.0/>).

1. Introduction

The biorefinery sector plays a crucial role in energy transition as it uses technologies to convert lignocellulosic biomass (LCB), once considered as waste, into renewable fuels. Lignocellulosic biomasses are mainly composed of agricultural and forest residues, but the main challenge in using lignocellulosic residues as raw materials is the need for a

pretreatment step [1,2]. This step is the most energy-intensive stage and accounts for more than 40% of the total production cost, while 30–50% is for the total equipment cost and 20–25% for the operational cost when lignocellulosic biomass is converted into biofuels such as bioethanol [3,4]. The high cost is due to the difficulty of breaking down the lignocellulose complex during the pretreatment. Lignocellulose (lignin, cellulose, and hemicellulose), which is the main component of plant cell walls, acts as the plant's natural defense system against various forms of aggression and also provides rigidity to plant cells [5]. In particular, lignin plays a crucial role in binding cellulose and hemicellulose together, but also prevents access to carbohydrates, making the pretreatment more difficult.

Various technologies for lignocellulosic biomass pretreatment have been developed with varying degrees of success. However, when integrated for the conversion of lignocellulosic biomasses into biofuels, these technologies fail to ensure the economic viability of the valorization. In other words, the cost per liter of the obtained biofuel remains higher than the market price, allowing fossil fuels to maintain a monopoly position [6,7]. In comparison, the cost of bioethanol production from sugar or starch-based feedstock (which is first-generation bioethanol) is a 43% lower compared to ethanol production from lignocellulosic biomasses (second-generation bioethanol) [8]. Nevertheless, 1G bioethanol is still less competitive compared to fossil fuels in general [9], although 2G bioethanol represents less than 5% of the global bioethanol production [10] and numerous technical and economic analyses have identified the pretreatment stage as the limiting factor in the valorization of lignocellulosic biomass [11,12]. This is why investigations on promising pretreatment methods are still ongoing. Reactive extrusion is one of these technologies [13]. Extrusion is a well-known thermomechanical process used in the plastics industry to mix and shape polymers. It was recently used as a physical pretreatment for lignocellulosic biomasses, especially using twin-screw extruders for good mixing conditions (materials uniformity) [14,15]. The biomass is fed into the extruder, where it undergoes high shear forces as it is conveyed from one end of the screws to the other. The shear is maximized through the design of the screw modules and temperature control. Some extruders are equipped with liquid injection ports, which are useful for materials with unsuitable rheological behavior, such as lignocellulosic biomasses (reactive extrusion) [16]. Extrusion is considered an attractive alternative to traditional pretreatment methods due to several advantages including high pretreatment speed, low operating and energy costs, low water consumption, non-selectivity of the biomasses, absence of inhibitor generation, and flexibility [17,18]. However, the success of extrusion strongly depends on choosing the right extrusion conditions, which presents a challenge due to the numerous parameters involved.

Extrusion conditions can be classified into three categories: intrinsic extruder parameters, biomass-related parameters, and operating parameters. Intrinsic extruder parameters include the number, size, type, configuration, and length of the screws, as well as the presence or absence of a die, and the die shape (metal channels imparting a specific cross-sectional shape to a polymer stream) [19]. Biomass-related parameters are the type of biomass, lignocellulosic composition, particle size, and moisture content. As for the operating parameters, they include temperature, screw rotation speed, biomass feed rate, biomass residence time, and recirculation. When a liquid chemical is injected during extrusion, a fourth category of parameters must be considered. These are the type of additive, concentration, injection rate, and injection location along the extruder barrel. Optimizing all these extrusion parameters is crucial to maximize the process performance.

This study had two consecutive objectives: (i) The optimization of the extrusion pretreatment for maximum delignification, and (ii) the analysis of the characteristics of the extrudates, to propose either a complementary pretreatment coupling for further delignification for LCB valorization into cost-effective bioethanol production, or the proposition of

possible biocomposite materials based on the results of the analysis. The study investigated the effects of reactive extrusion on lignocellulosic biomasses in terms of delignification percentage and structural characteristics of the resulting extrudate. Corn stover (agricultural residue) and black spruce residues (forestry residues) were selected as feedstocks for this study. Corn is the primary crop in Quebec province (Canada) and black spruce is one of the main tree species. According to the last report of the Ministry of Energy and Natural Resources of Quebec, about 6.8 million tons/year of wood and 549,000 tons/year of agricultural residues are available in the province for bioenergy production [20].

2. Materials and Methods

2.1. Raw Biomasses and Characterization

One forest residue and one agricultural residue were used in this work: black spruce (*Picea mariana*) and corn stover (*Zea mays*). Black spruce chips (BS) were provided by Savard et Fils sawmill (Quebec, QC, Canada), and dry corn stover (CS) was provided by Agrosphere Inc. (Quebec, QC, Canada). BS consisted exclusively of chips from the tree trunk, while CS consisted of a mixture of leaves, stalks, and cobs. Upon receipt, BS and CS had particle sizes between 2 and 5 mm. They were ground into 1 mm and 1.5 mm (for extrusion trials) using a Pulverisette 15 (Frisch, Idar-Oberstein, Germany) and stored at room temperature. A sample of each biomass was ground with a small grinder (Magic Bullet, Toronto, ON, Canada), and particle size below 0.2 mm was collected for characterization, especially to determine the biomass composition in terms of cellulose, hemicellulose, lignin, and extractives. Extractives and hemicellulose were determined using NDF (Neutral Detergent Fiber) and ADF (Acid Detergent Fiber) method respectively, using an ANKOM fiber analyzer (ANKOM, Macedon, NY, USA) [21]. Finally, the lignin content was evaluated using the Klason Lignin method, while cellulose content was calculated by mass comparison [22].

2.2. Parameter Screening

Pretreatment parameters were screened by: (i) extensive literature reviews summarized in Konan et al. [19,23], (ii) through preliminary extrusion trials, and (iii) operation constraints. Table S1 (Supplementary Material) presents the details of the parameters selection.

2.3. Reactive Extrusion

The reactive extrusion steps were performed using a Process 11 extruder (Thermo Scientific, Waltham, MA, USA) equipped with twin co-rotating screws (11 mm diameter each). The standard screw configuration was used for all extrusions. It consisted of four (4) forward screw zones and three (3) kneading element zones as shown in Figure 1. Before extrusion, some amounts of each biomass were mixed with sodium hydroxide according to the experimental plan (Section 2.3). The trials of the experimental plan were randomly performed. For each trial, 20 g of extrudates were collected only when the conditions (temperature, screw speed, and torque) were stable. Daily extrusion trials were preceded and followed by cleaning (purging) the extruder with low-density polyethylene (LDPE).

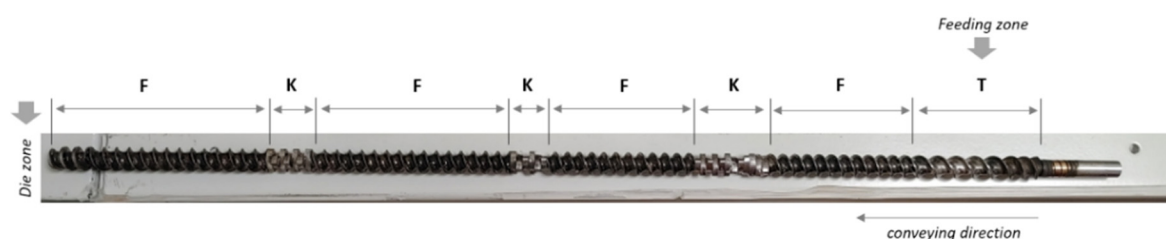


Figure 1. Screw configuration for the extrusion step (T = transport zone, F = forward screw element, and K = kneading blocks).

2.4. Experimental Plan

Prior to the experimental plan, multiple series of trials were run in different extreme conditions of temperature, rotation speed, particle size, biomass moisture, biomass/NaOH ratio, biomass feeding throughput, extruder die configuration, feeding ratio, and biomass recirculation to determine the experimental space. This resulted in different experimental spaces for BS and CS as shown in Table 1. Then, a faced central composite design (CCD) was designed with Design Expert 13 software to build the experimental plan for each biomass. The central composite design was chosen for its flexibility (ex: more trials can be added if needed) and robustness to estimate complex interactions and non-linear effects between parameters which was expected with biomass extrusion and confirmed by this study. However, the choice of the faced-centered central composite design (FCCCD) instead of the rotatable central composite design (RCCD) was dictated by preliminary experiments. It was not possible to extrudate the biomasses beyond the experimental space (ex: screw speed < 150 rpm or >300 rpm) so α (the distance of axial points from the center) was equal to 1. The experimental plan for each biomass is composed of 34 runs including 6 center points (Table 2).

Table 1. Experimental space for the extrusion conditions.

	Black Spruce Chips (BS)				Corn Stover (CS)			
	Screw Speed	Temp	NaOH	Particle Size	Screw Speed	Temp	NaOH	Particle Size
Type	Numeric	Numeric	Numeric	Categoric	Numeric	Numeric	Numeric	Categoric
Unit	rpm	°C	%	mm	rpm	°C	%	mm
Low level (−1)	150	50	0	1	80	40	0	1
High level (+1)	300	100	15	1.5	300	110	15	1.5
− alpha	150	50	0	1	80	40	0	1
+ alpha	300	100	15	1.5	300	110	15	1.5

Table 2. Experimental trials for black spruce chips (BS) and corn stover (CS).

Run	Black Spruce Chips				Corn Stover			
	Screw Speed (rpm)	Temp (°C)	NaOH ¹ (%)	Particle Size (mm)	Screw Speed (rpm)	Temp (°C)	NaOH (%)	Particle Size (mm)
1	300	100	0	1	190	80	7.5	1.5
2	225	50	7.5	1	190	80	15	1.5
3	150	100	0	1.5	190	80	15	1
4	300	50	0	1.5	80	110	0	1.5
5	150	50	15	1.5	300	50	0	1.5
6	300	75	7.5	1.5	190	80	0	1
7	150	75	7.5	1	80	80	7.5	1.5
8	225	50	7.5	1.5	80	110	0	1
9	150	50	0	1	190	80	7.5	1
10	300	100	0	1.5	80	80	7.5	1
11	225	75	7.5	1	300	80	7.5	1
12	300	50	0	1	80	50	15	1.5

Table 2. *Cont.*

Run	Black Spruce Chips				Corn Stover			
	Screw Speed (rpm)	Temp (°C)	NaOH ¹ (%)	Particle Size (mm)	Screw Speed (rpm)	Temp (°C)	NaOH (%)	Particle Size (mm)
13	225	75	7.5	1	80	50	15	1
14	150	50	15	1	300	50	0	1
15	150	100	0	1	190	50	7.5	1.5
16	225	75	7.5	1.5	190	110	7.5	1.5
17	300	50	15	1	300	110	15	1
18	225	100	7.5	1	190	80	7.5	1
19	300	100	15	1.5	80	110	15	1
20	300	50	15	1.5	300	110	0	1.5
21	225	75	0	1	80	50	0	1.5
22	300	100	15	1	190	80	7.5	1.5
23	225	75	0	1.5	300	110	15	1.5
24	300	75	7.5	1	300	50	15	1
25	150	100	15	1.5	300	110	0	1
26	225	75	15	1.5	190	80	7.5	1.5
27	225	75	7.5	1.5	300	50	15	1.5
28	150	50	0	1.5	190	50	7.5	1
29	225	75	7.5	1	80	50	0	1
30	150	75	7.5	1.5	190	80	7.5	1
31	225	75	15	1	80	110	15	1.5
32	150	100	15	1	190	80	0	1.5
33	225	75	7.5	1.5	190	110	7.5	1
34	225	100	7.5	1.5	300	80	7.5	1.5

¹ 0% NaOH indicates that the biomass has only been mixed with water.

2.5. Preparation of Biomass

The additive used was sodium hydroxide (NaOH) 98% purity purchased from Thermo Scientific (USA). The NaOH solutions were mixed with the biomass just before extrusion with an additive ratio of 2:1 (*w/w*). For instance, 500 g of biomass was mixed with 250 g of water or NaOH solution (7.5% or 15% *w/w* NaOH) according to the experimental plan (Table 2).

2.6. Moisture Content

The moisture content of the extrudates was determined using a moisture analyzer HR83 Halogen (Mettler Toledo, Mississauga, ON, Canada) as follows: 0.5 g of the extrudate was placed in the apparatus and heated to 105 °C until the mass of the sample remained constant (5–10 min). The moisture content was then calculated as:

$$\text{Moisture} = \frac{0.5 - m_{105}}{0.5} (100) \quad (1)$$

where m_{105} is the constant mass of biomass when heated at 105 °C.

2.7. Particle Size and Specific Surface Area

Particle size distribution and specific surface area of the extrudates and the raw materials were measured using a laser scattering analyzer Horiba LA-950 (Horiba Ltd., Kyoto, Japan).

2.8. Delignification Percentage

Before delignification analysis, the extrudates were filtered with hot water several times until neutral pH to remove sodium hydroxide and the soluble products of lignin degradation. The filtered extrudates were then oven-dried at 50 °C. The insoluble lignin composition of the biomass was determined by the Klason method. In a 100 mL beaker, 0.5 g of biomass was added along with 20 mL of 72% sulfuric acid (H₂SO₄) solution prepared from 98% H₂SO₄ (Fisher Chemicals, Ottawa, ON, Canada). The content of the beaker was stirred at regular intervals for 1 h and 20 min. Afterward, the mixture was transferred to a 320 mL round-bottomed cylindrical tube and 290 mL of distilled water was added to obtain a 3% H₂SO₄ solution. The tube was then placed in a digester and heated to 185 °C for 3 h. The content was filtered and washed with 200 mL of distilled water using a filter device and Whatman 45 µm paper. The solid fraction on the Whatman paper was placed in a 100 mL beaker and dried overnight at 105 °C. Once dried, the beaker was weighed, and the dry mass of insoluble lignin (biomass dry solid fraction) was calculated by subtracting the weight of the filter paper and the beaker (which were weighed beforehand). The delignification percentage was calculated by comparing the mass of lignin in the raw biomass to the mass of lignin in the extrudate. The equation for the delignification percentage is:

$$\gamma = \frac{mL_{\text{raw}} - mL_{\text{ext}}}{mL_{\text{raw}}} (100) \quad (2)$$

where mL_{raw} represents the mass of lignin in the raw biomass, while mL_{ext} represents the mass of lignin in the extrudate.

2.9. Optimization

BS and CS were optimized separately due to their different experimental space. The optimizations were performed by using the response surface methodology (RSM). RSM uses mathematical and statistical methods to predict a dependent variable based on a set of independent variables and a regression equation (see Equation (3)). The extrusion conditions were mathematically modeled into a regression equation to match their respective results. Then, by calculating appropriate statistical tests, such as the variance ratio (F) and the associated *p*-value (probability), the analysis of variances (ANOVA) was used to determine by iteration the effect of each term on the final response. The terms that did not meet the significance thresholds were removed from the model to refine it. Once the model was obtained, it was possible to identify the best response that could be achieved within the defined experimental space. The input parameters in this study were the particle size (mm), screw rotation speed (rpm), temperature (°C), and sodium hydroxide concentration (% *w/w*). The main response investigated was the delignification percentage, while the secondary responses were the specific surface area and the particle size of the extrudates. The general equation for a quadratic model with *n* independent variables is provided by:

$$y = \beta_0 + \beta_1 X_1 + \beta_2 X_2 + \dots + \beta_n X_n + \beta_{11} X_1^2 + \beta_{22} X_2^2 + \dots + \beta_{nn} X_n^2 + \beta_{12} X_1 X_2 + \dots + \beta_{1n} X_1 X_n + \beta_{2n} X_2 X_n + \varepsilon \quad (3)$$

where *y* is the response, *X*₁, *X*₂, ..., *X*_{*n*} represent the independent variables, β_0 represents the intercept term, $\beta_1, \beta_2, \dots, \beta_n$ are the coefficients of the linear terms, $\beta_{11}, \beta_{22}, \dots, \beta_{nn}$

are the coefficients of the squared (quadratic) terms, $\beta_{12}, \beta_{13}, \dots, \beta_{1n}, \beta_{2n}$ are the interaction coefficients, and ε represents the experimental error.

2.10. Scanning Electron Microscopy (SEM)

The morphology of the biomass was examined before and after extrusion using scanning electron microscopy (SEM) (Zeiss EVO[®] 50 smart SEM, Oberkochen, Germany). Different magnifications (Mag) and working distances (WD) were used, along with a secondary electrode 1 (SE 1) detector and an Extra High Tension (EHT) of 10 kV. Prior to SEM testing, all the samples were coated with a fine platinum layer using a High Vacuum Sputter Coater (Leica Microsystems, Richmond Hill, ON, Canada).

2.11. Fourier Transformed Infrared Spectroscopy (FTIR) Analysis

FTIR spectra for the raw and extruded biomasses were recorded with a Nicolet iS50 FT-IR spectrophotometer equipped with a standard ATR crystal cell detector (Thermo Scientific, Waltham, MA, USA). The wavelength range was from 400 to 4000 cm^{-1} . Each spectrum was acquired by the average of 16 scans with 4 cm^{-1} resolution.

2.12. Gas Chromatography/Mass Spectrometry (GC/MS)

After optimizing the extrusion conditions, 2 g of biomass was sampled from the extrudate and blended with 40 g of deionized water into a 250 mL beaker. The mixture was thoroughly mixed and slightly heated for 5 min on a heated plate equipped with magnetic stirring. After 5 min, the mixture was filtered with a 45 μm Whatman paper. The filtrate was collected and injected in a Clarus 500 Gas chromatography/mass spectrometry (Perkin Elmer, Shelton, CT, USA). Sample injection was performed in splitless mode, with an injector temperature of 250 $^{\circ}\text{C}$, a splitless time of 0.75 min, and an injection volume of 0.7 μL . Water was used as the rinsing solvent for both injectors A and B. Chromatographic separation was carried out on a RTX-WAX column (30 m \times 0.25 mm \times 0.25 μm), with a constant helium flow rate of 1.5 mL/min as the carrier gas. The initial oven temperature was set to 70 $^{\circ}\text{C}$. Detection of the compounds was performed in SCAN mode with a mass range of 35–350 m/z , a transfer line temperature of 250 $^{\circ}\text{C}$, and an ion source temperature of 260 $^{\circ}\text{C}$.

3. Results and Discussion

3.1. Biomass Characteristics

Figure 2 displays the elemental compositions of raw BS and raw CS in terms of carbon (C), hydrogen (H), nitrogen (N), and sulfur (S). These two biomasses have similar compositions, in terms of the relative proportion of each four chemical elements and in terms of the CHNS percentage. Sulfur in both biomasses was too low to be detected as well as nitrogen in BS. CHNS represents 53.7% of the total mass of BS and 50.3% of CS. The relative proportion of each element influences the calorific value of the biomass. Theoretically, BS and CS have similar calorific values. Based on Equation (4) given by [24], the calorific values are respectively 19.3 MJ/kg and 18.7 MJ/kg. However, in terms of cellulose, hemicellulose, lignin, extractives, and ash composition, both biomasses exhibit different compositions (Figure 3). The relative proportion of these compounds is more balanced in CS than in BS, meaning that the variance in BS components is significantly higher than in CS (resp. 264.3 and 90.1). The lignin content of BS is $28.9 \pm 0.7\%$, which is 1.5 times higher than the lignin content of CS ($18.9 \pm 0.7\%$). Similarly, BS contains almost twice the cellulose amount in CS, but less than half its hemicellulose content. The high level of extractives in CS is explained by the mixed composition of these residues. They consist of various parts of the plant, including peduncles, spathes, stigmas, panicles, stems,

and leaves. These parts contain varying amounts of crude protein and starch, known as non-structural components (NSC) [25]. They can be up to 30% in corn stover [26]. NSCs are soluble in neutral detergent. They are all removed at the NDF (Neutral Detergent Fiber) stage in the Van Soest method and accounted as extractives [27,28]. These characterization results are coherent with those of Fang et al. [29] for BS and Zhang et al. [26] for CS.

$$CV = -1.3675 + 0.3137C + 0.7009H + 0.0318O^* \quad (4)$$

where CV: calorific value (MJ/kg), C: Carbon proportion (%), H: Hydrogen (%) and O*: O = 100 – C – H – Ash.

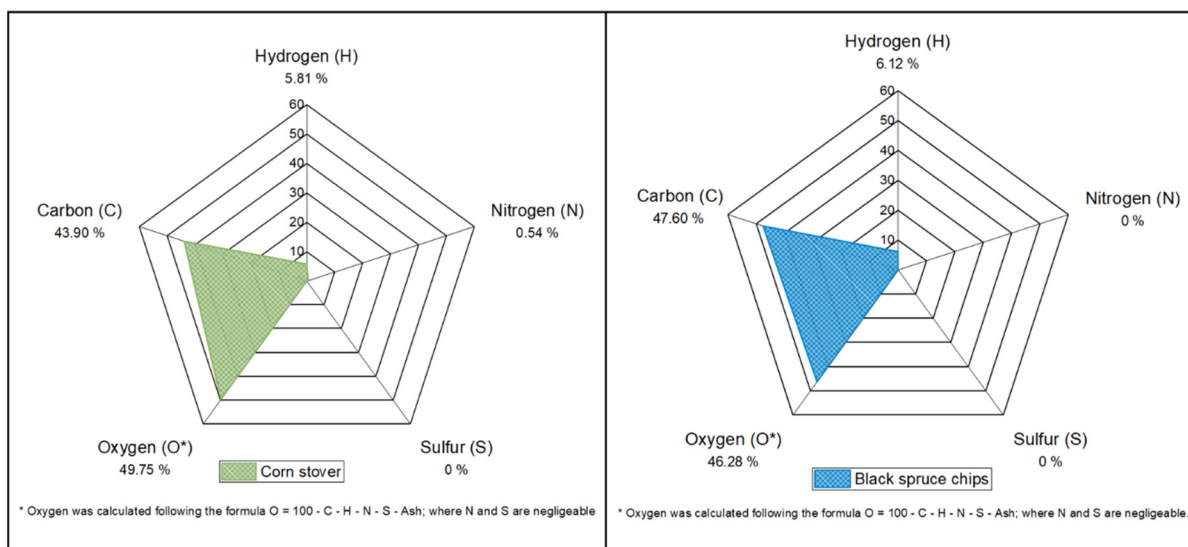


Figure 2. Elemental composition of black spruce chips and corn stover.

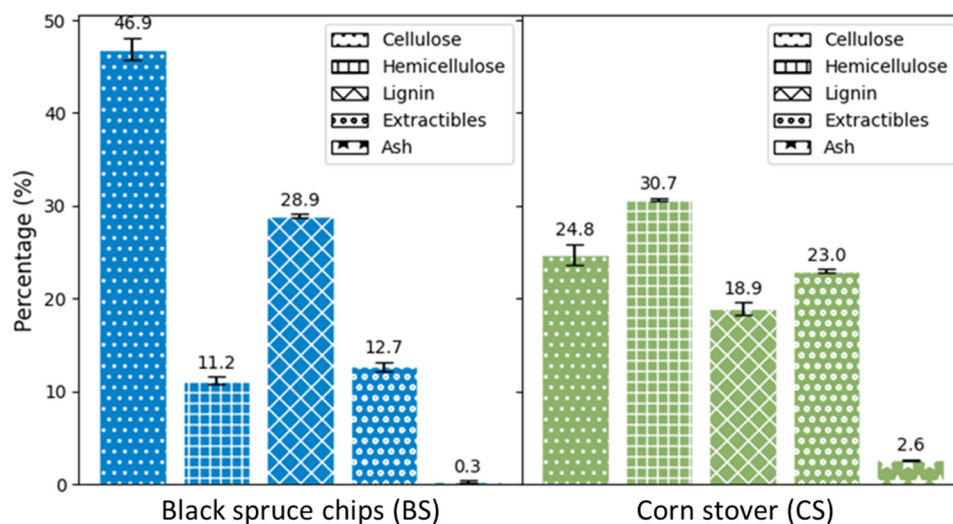


Figure 3. Black spruce chips (BS) and corn stover (CS) characterization.

3.2. Extrusion Conditions

Screw configuration is an important parameter for an efficient pretreatment of ligno-cellulosic biomass by extrusion. The screw configuration used in this study was based on previous literature data [19]. It consisted of three kneading zones (K), four forward conveying zones (F), and one transport zone (T) (also the biomass feeding zone) (Figure 1). No reverse screw elements were included in the configuration to avoid excessive pressure

in the extruder, pore blocking, and lignin redistribution in the biomass, as observed by Zheng et al. [30].

Biomass structural compositions (lignin, cellulose, and hemicellulose) do have an impact on extrusion conditions. Preliminary tests conducted to determine the experimental space led to different temperature and rotation speed conditions for BS and CS (Table 3). Trials were initially conducted with two dies of different sizes (diameters of 1 mm and 3 mm) to maximize the back pressure in the barrel but were later repeated without them. The dies obstructed the extrudates from exiting properly and the extrudates were compacted by the screw behind the die. This was then often followed by the jamming of the screws. The compaction behind the die was especially fast when the extrusion trials involved sodium hydroxide solution such as in runs 2, 5, and 6 (Figure 4). Sodium hydroxide is a strong alkaline agent that depolymerizes lignin in the biomass, making the fibers more susceptible to deformation and stretching [31]. Under pressure and elevated temperature, sodium hydroxide becomes viscous and easily mixes with the biomass. However, the change in temperature and pressure at the extruder outlet solidified it, causing the NaOH to function as a binder, holding the CS particles together. As for BS, extrusions with dies were impossible due to extruder jamming. Using a die may also affect the cost and energy balance of the pretreatment, as it requires an additional grinding step of the extrudate before subsequent processing steps such as washing or enzymatic hydrolysis. In line with these results, all the 68 trials (34×2) were performed without dies.

Table 3. Extrusion experimental space codes.

Parameters	Black Spruce Chips		Corn Stover	
	Low Level (−1)	High Level (+1)	Low Level (−1)	High Level (+1)
Screw speed (rpm)	150	300	80	300
Temperature (°C)	50	100	40	110
NaOH (% <i>w/w</i>)	0	15	0	15
Particle size (mm)	1	1.5	1	1.5

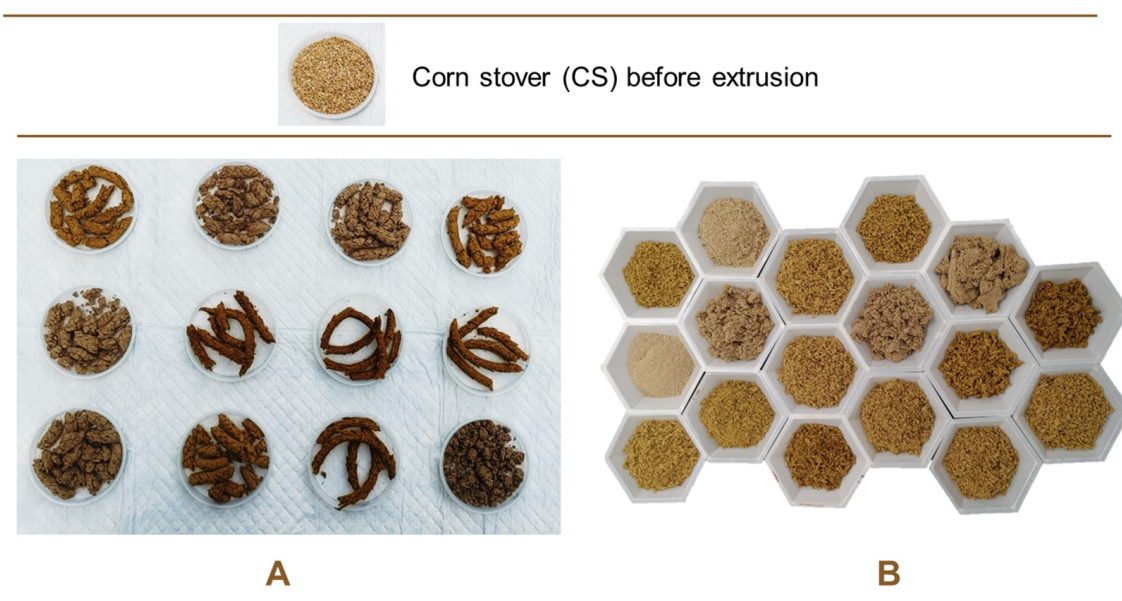


Figure 4. Corn stover of 1 mm particle size extruded: (A) with a die, and (B) without a die.

The minimum screw rotation speed for BS was 150 rpm, and 80 rpm for CS (Table 3). CS are more compressible than BS which has more rigid particles. Below 150 rpm for BS

and 80 rpm for CS, the torque required to set the screws in motion exceeds the extruder's capacity, causing the screws to stop. On the other hand, above 300 rpm for both biomasses, the speed was too high and created an instability in the rotation of the screws. This instability caused the co-rotation to become less synchronous and the screws to jam. There are two main reasons for this instability. First, the rheological behavior of biomasses, unlike most polymers, is random due to the irregular shape of their particles. Secondly, the biomass is discontinuous along the screws because most of the load is blocked in the kneading zones. In fact, at higher speeds, the residence time of the extrudate in the mixing element where the kneading occurs and where the shear forces are maximal is shortened. Therefore, the particle sizes are not sufficiently reduced to be convoyed from the first mixing element to the next element while new biomass loads are pushed into the mixing zone by the previous screw elements. This creates a load difference between the mixing zones and instability in the twin-screw synchronous rotation. These results indicate that the type and composition of biomass can significantly affect extrusion conditions, specifically screw rotation speed. Therefore, it is crucial to conduct preliminary extrusion tests for each new biomass. Regarding the difference in temperature range, it was greater with CS than with BS. This is attributed to the hygroscopic properties of agricultural residues as they tend to internally absorb more moisture compared to forest residues. The internal moisture content affects the biomass thermal behavior during processing. The higher the moisture is, the more important the biomass compression and the hot water effect on the fibers. It has also been observed that water evaporated during extrusion, even though the boiling point of water is beyond the barrel temperature due to high pressure. This phenomenon is governed by Equation (5) the Clausius-Clapeyron equation, which describes the relationship between vapor pressure and temperature [32]. In the mixing zones, the real-time temperature was higher than the setpoint temperature due to the high shear forces occurring there. Under these conditions, the water vapor pressure also increases, resulting in a sudden release of water molecules in steam form.

$$\ln\left(\frac{P_1}{P_2}\right) = -\frac{\Delta H_{vap}}{R}\left(\frac{1}{T_1} - \frac{1}{T_2}\right) \quad (5)$$

where P_1 is the vapor pressure at temperature T_1 ; P_2 is the vapor pressure at temperature T_2 ; ΔH_{vap} is the enthalpy of vaporization of the substance; and R is the ideal gas constant (8.314 J/mol K).

3.3. Extrudate Characteristics

After each extrusion trial (68 in total), the delignification percentage, moisture, particle size, and specific surface area of the extrudates were measured. These parameters represent the four responses (S1 to S4) for BS and (R1 to R4) for CS.

Moisture is an important parameter not only for operational reasons as it allows a steady flow (stability) of the extrusion, but is also important for the reduction of water consumption during downstream processes; higher moisture is better. However, the moisture of the trials varied widely, ranging from 23.6% to 59.2% for R2 and from 5.4% to 34.8% for S2. These results indicate that BS retains moisture better during extrusion compared to CS although they absorb less comparatively, as reported in Section 3.2. Pearson coefficient analysis was performed to assess the relationship between the parameters [33,34]. Table 4 present the correlation matrix. For black spruce extrudates (BSE), there is no statistical evidence supporting a correlation between the extrusion temperature and the extrudate moisture ($r = -0.283$, $p > 0.05$) or between the screw speed and the extrudate moisture ($r = -0.021$, $p > 0.05$). However, the sodium hydroxide concentration and the extrudate moisture are positively related ($r = 0.349$, $p < 0.05$). Lower moisture seems to

be influenced by a combination of both temperature and NaOH concentration. On the other hand, for corn stover extrudates (CSE), the significant moisture loss was negatively correlated with the extrusion temperature ($r = -0.719$, $p < 0.05$), as well as with the specific surface area ($r = -0.753$, $p < 0.05$). The higher the temperature, the higher the specific surface and the lower the moisture. In addition, particle size and specific surface area are negatively correlated ($r = -0.849$, $p < 0.05$). This can be explained by the fact that CSE particles agglomerate with moisture, resulting in larger particles and reduced specific surface area.

Table 4. Pearson correlation coefficients.

Corn stover								
	S.S	T °C	[NaOH]	P.S ⁺	D %	M %	S.S.A	E.P.S
Screw speed (S.S)	1.000	0.000	0.000	n.a	0.037	0.027	−0.007	0.022
Temperature (T °C)		1.000	0.000	n.a	−0.144	−0.719 *	0.298	−0.145
[NaOH]			1.000	n.a	0.070	0.078	−0.312	0.577 *
Particle size (P.S)				n.a	n.a	n.a	n.a	n.a
Delignification (D %)					1.000	−0.029	0.134	−0.013
Moisture (M %)						1.000	−0.753 *	0.548 *
Specific surface area (S.S.A)							1.000	−0.849 *
Extrudate particle size (E.P.S)								1.000
Black spruce								
	S.S	T °C	[NaOH]	P.S	D %	M %	S.S.A	E.P.S
Screw speed (S.S)	1.00	0.00	0.000	n.a ⁺	0.302	−0.021	−0.285	0.285
Temperature (T °C)		1.00	0.000	n.a	−0.015	−0.283	−0.027	−0.053
[NaOH]			1.000	n.a	0.314	−0.349 *	−0.106	0.200
Particle size (P.S)				n.a	n.a	n.a	n.a	n.a
Delignification (D %)					1.00	−0.105	−0.076	0.191
Moisture (M %)						1.00	0.120	−0.190
Specific surface area (S.S.A)							1.00	−0.957 *
Extrudate particle size (E.P.S)								1.00

⁺ categoric parameter, * p -value inferior to 0.05.

The particle sizes of all extrudates ranged from 68 to 205 μm for BSE (S3) and from 116 to 1204 μm for CSE (R3). Raw BS particle sizes (1 mm and 1.5 mm) did not have a significant effect on their extrudate particle sizes (Figure 5). On the contrary, for CS, there was an important size difference between the initial particle sizes and their resulting CSE particles. The median CSE particle sizes were 328 μm and 713 μm respectively for CS 1 mm and CS 1.5 mm, which were much higher than those of BSE (122 μm and 148 μm). The extrudate particle size distribution with raw residues grounded with a fine grinder (Magic Bullet, Québec, Canada) was also done to investigate the difference in size reduction between extrusion and grinding. Figure 6A,B present the results on logarithmic scales. With grinding, it was not possible to achieve more particle size reduction even after several cycles and/or for a longer duration than the extruder takes. This is because the shear forces in the kneading zones are responsible for the mechanical reduction in particle size. In this zone, intensive grinding occurs under pressure in a confined space (with a clearance in the microns range), which is not the case in a grinder. For particle size reduction, extrusion has

the advantage of being very fast as it takes between a few seconds to 2 min for biomass to move from the feeding zone to the die exit (Table 5).

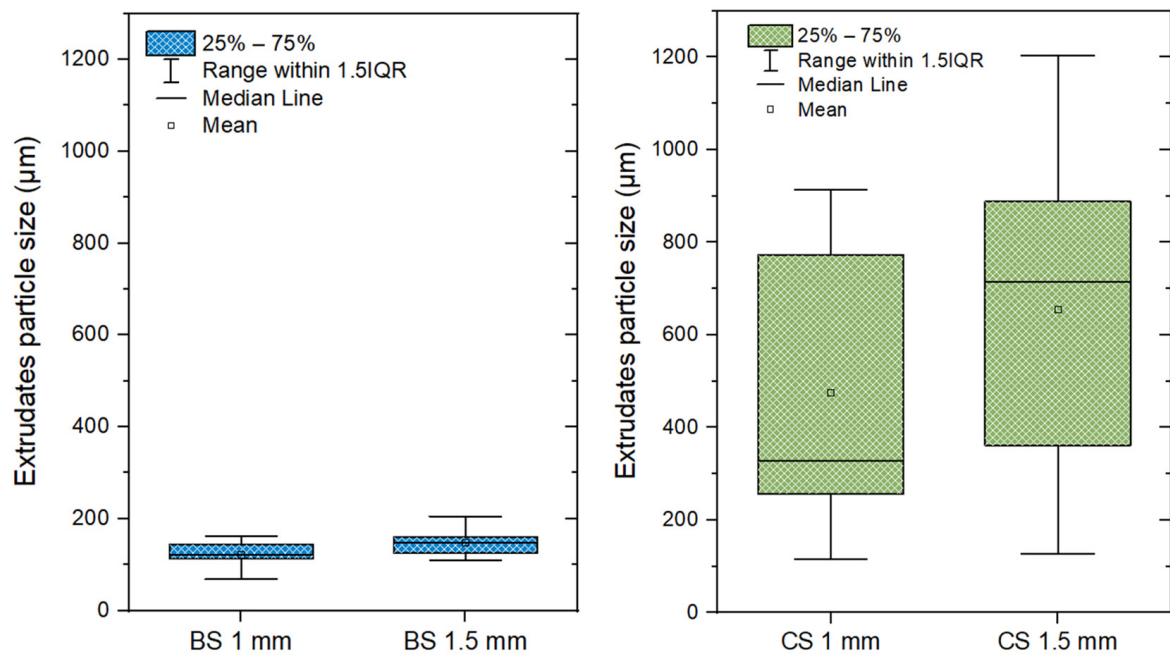


Figure 5. Distribution of the extrudate particle size (black spruce chips and corn stover).

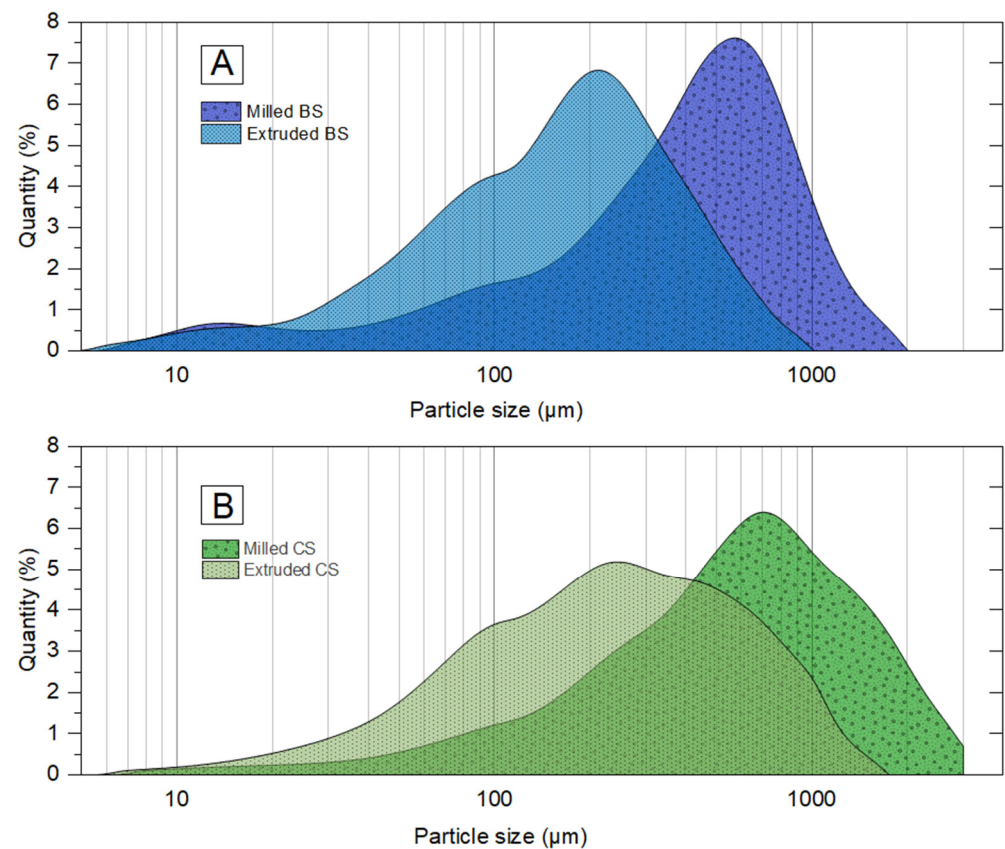


Figure 6. Comparison of the particle size distribution between the extrudates and milled raw biomasses: (A) black spruce chips (BS), and (B) corn stover (CS).

Table 5. Summary of the responses obtained.

Response	Parameter	Units	Observations	Minimum	Maximum	Mean	Std. Dev.	Ratio
Corn Stover Extrudates (CSE)								
R1	Delignification	%	34	2.2	24.4	12.7	6.1	10.9
R2	Moisture	%	34	5.4	34.8	25.1	8.3	6.4
R3	Particle size	µm	34	115	1203	565	324	10.4
R4	Specific surface area	cm ² /cm ³	34	174	1183	462	271	6.8
Black Spruce Extrudates (BSE)								
S1	Delignification	%	34	0.9	25.2	12.6	4.5	25.8
S2	Moisture	%	34	23.6	59.2	31.8	5.6	2.5
S3	Particle size	µm	34	68.2	204	135	29	3.0
S4	Specific surface area	cm ² /cm ³	34	646	1569	955	203	2.4

3.4. Statistical Analysis

A design of experiments is used to model a phenomenon, process, procedure, or response reliably and robustly, based on a reduced number of trials. The benefit is that it saves time, energy, and money [35]. A design of experiments is generally used for one of three purposes: (i) comparison or characterization, (ii) screening, and (iii) optimization. A comparison or characterization design is used to confirm the importance of a parameter on the response, independently of their important parameters. Screening is used to identify which parameters have the highest influence on the response [36]. Optimization is by far the most widespread of all, it is used to determine the optimal configuration(s) of parameters according to the desired level of response. In practice, optimization is often preceded by screening, which can also be a literature review validated by experimental data, such as in this study [19].

The objective of this study was to optimize the pretreatment conditions of lignocellulosic biomass to achieve the highest possible delignification percentage. Therefore, delignification was the main response. Table S2 (Supplementary Material) reports the results of the experimental plans including the delignification percentages. The delignification percentage ranges between 2.2% and 23.5% for R1 (CS) and from 1% to 25.3% for S1 (BS). These significant variations in delignification percentage justified the need for an optimization of the extrusion conditions. Table S2 also includes six center points per biomass (three center points for 1 mm residues and three for 1.5 mm residues). A center point refers to a point at the center of the experimental space, which is repeated multiple times independently under the same conditions to validate the reproducibility of the results. The highest standard deviation recorded for delignification percentages at center points was 1.2% (CS with 1 mm). This result suggests that the accuracy of the delignification data in the table is $\pm 1.2\%$, which is very good considering the complex situation analyzed. The best delignification achieved with BS was with BS 1 mm, extruded at 225 rpm, without sodium hydroxide, and at 75 °C. For CS, the best percentage was obtained with CS 1 mm, extruded at 300 rpm, without sodium hydroxide, and at 50 °C. So, the best conditions seem to be obtained with small particle sizes, high screw rotation speeds, low temperatures, and without NaOH. These results partially differ from our expectations, especially for the effect of sodium hydroxide. It was expected that its presence would help the delignification step of the biomass due to its ability to depolymerize lignin and break lignin-hemicellulose bonds [37,38]. The assumption was supported by the 2nd best results (22.3% for BS and 23.7% for CS), but not for the optimum results. The 2nd best results were obtained when the biomasses were extruded with a 15% *w/w* NaOH solution. However, these results could be

explained by the fact that lignin can recondense or form a pseudo-lignin complex under harsh alkaline conditions and high temperatures [39]. Komatsu and Yokoyama [40] also observed lignin recondensation above 130 °C, which is likely to occur during extrusion due to shear forces locally increasing the thermal energy (viscous dissipation) in the biomass.

The results in Table S1 were used to determine the regression equations to model the delignification percentages of both biomass ($Y_1 = \text{BS}$ and $Y_2 = \text{CS}$) as a function of the parameters studied ($A = \text{screw rotation speed}$, $B = \text{temperature}$, $C = \text{NaOH concentration}$, and $D = \text{particle size}$). Equations (6) and (7) respectively model the delignification responses of black spruce (S1) and corn stover (R1) as:

$$Y_1 = 12.09 + 1.77A - 1.04AC - 1.47AD - 2.24BC + 4.17BD + 2.14CD + 4.99C^2 + 0.5813ABC + 1.01ABD - 0.5725BCD + 2.38A^2C - 1.39A^2D - 1.2B^2D - 5.75C^2D + 0.585ABCD - 4.98A^2B^2 - 5.16A^2BD - 1.89A^2CD - 1.89A^2CD + 9.29A^2B^2D \quad (6)$$

$$Y_2 = 11.51 + 4.62A + 1.57B - 2.41C + 1.94D - 2.01AB + 0.8169AC + 4.41CD - 1.75B^2 + 3.81C^2 + 1.12ABC - 2.37ABD - 1.33BCD - 3.38A^2B + 3.71A^2C - 6.71A^2D - 5.41AB^2 + 2.86B^2D - 2.9ABCD + 3.25A^2BD - 2.92A^2CD \quad (7)$$

For each model, an analysis of variance (ANOVA) was performed to evaluate its significance. Table 6 summarizes all the results. Both models successfully passed the p -values significance test ($p < 0.05$). The lack of fit is a measure of how well a model fits the data. In both cases, the p -values of the lack of fit did not pass the significance test ($p > 0.05$ for BS and CS). This indicates that both models fit well their respective data. A lack of fit less than 0.05 would indicate that the model predictions are significantly different from the observations [41]. To confirm the statistical tests, the delignification percentages predicted by the models were compared with the experimental delignification percentages (Figure 7). The predicted and experimental data fit well ($R^2 = 0.9865$ for the BS model and $R^2 = 0.9660$ for the CS model).

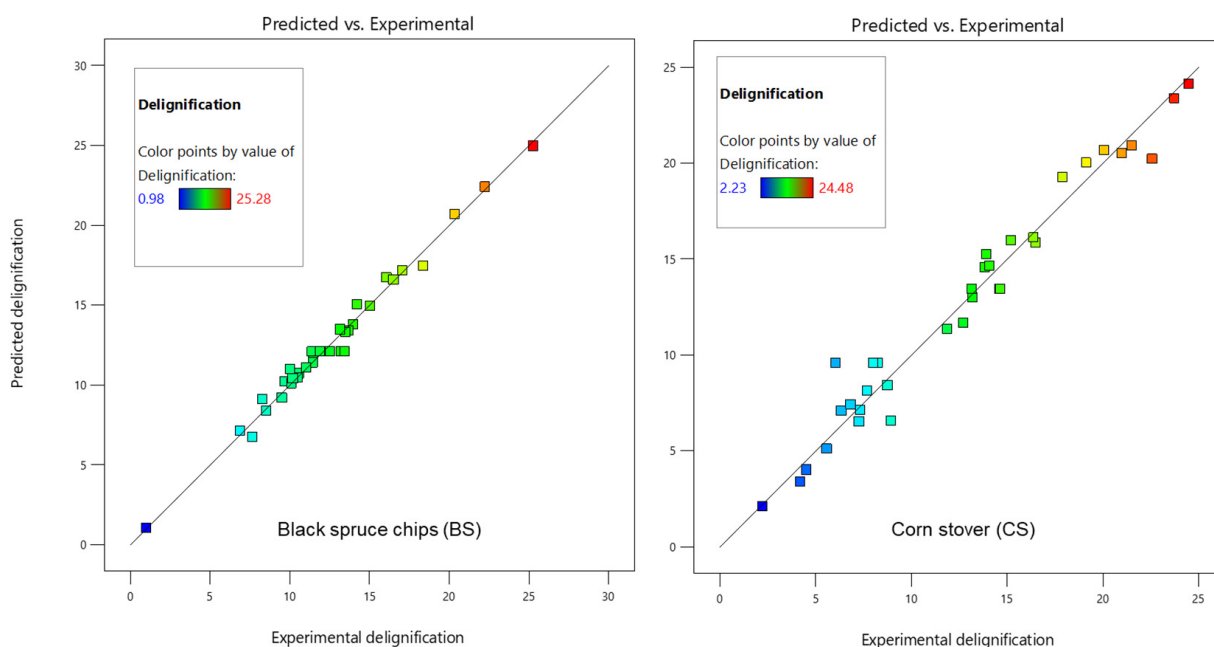


Figure 7. Model predictions as a function of the experimental delignification percentage.

Table 6. Summary of the ANOVA analysis for BS and CS.

Source	Sum of Squares	df	Mean Square	F-Value	p-Value	Significance
Black spruce chips						
Model	679.35	19	35.76	53.87	<0.0001	Significant
Residual	9.29	14	0.6637			
Lack of Fit	6.43	10	0.6426	0.8972	0.5977	Not significant
Pure Error	2.86	4	0.7162			
Cor Total	688.64	33				
Corn stover						
Model	1206.48	20	60.32	18.49	<0.0001	Significant
Residual	42.40	13	3.26			
Lack of Fit	38.03	9	4.23	3.87	0.1028	Not significant
Pure Error	4.37	4	1.09			
Cor Total	1248.88	33				

3.5. Effect of the Parameters on Delignification Percentage

Figure 8 shows the 2D and 3D response surfaces for the two best delignification conditions for BS and Figure 9 the same results for the two best delignification conditions for CS. For BS, the space delimited by the highest delignification percentages (in red) is larger than that of CS. The boundary conditions of temperature and rotation speed have a very significant effect on the delignification percentages of BS, which is not the case for CS. The highest delignification percentages for BS are in the 50–90 °C and 200–300 rpm range. For CS, a concentration of higher delignification percentages is observed in smaller zones delimited by 60–95 °C and 290–300 rpm. On the 2D plots for both biomasses and conditions, the screw rotation speed is the parameter with the highest influence on delignification percentages, at least more important than the temperature. Below 190 rpm, the probability of obtaining delignification percentages above 20% becomes lower. However, in practice, higher speeds can lead to process instability, especially with biomass containing high lignin contents (above 25%).

3.6. Response Optimization

Extrusion optimization consisted of finding the parameters that lead to the best delignification percentages for each biomass. It was based on the analysis of the response surfaces with Design Expert 13. The optimization constraints were: (i) minimize NaOH concentration to reduce pretreatment costs and chemical usage, (ii) minimize raw biomass particle size to avoid extruding under unstable conditions and damaging the equipment over time, (iii) minimize rotation speed to avoid extruder instability and reduce specific mechanical energy, (iv) minimize extrusion temperature to reduce costs and retain more biomass moisture during extrusion, and (v) ensure that the delignification percentage is above 20% as reported in the literature [42].

Table 7 presents the relative importance of each constraint. The optimization was conducted numerically using the Y_1 and Y_2 equations (Equations (6) and (7)) and the Design Expert software integrated solver. With these constraints, the solutions were under the following conditions:

For Y_1 (28.9%): A = 233 rpm, B = 50 °C, C = 0%, and D = 1 mm.

For Y_2 (26.6%): A = 300 rpm, B = 65 °C, C = 0%, and D = 1 mm.

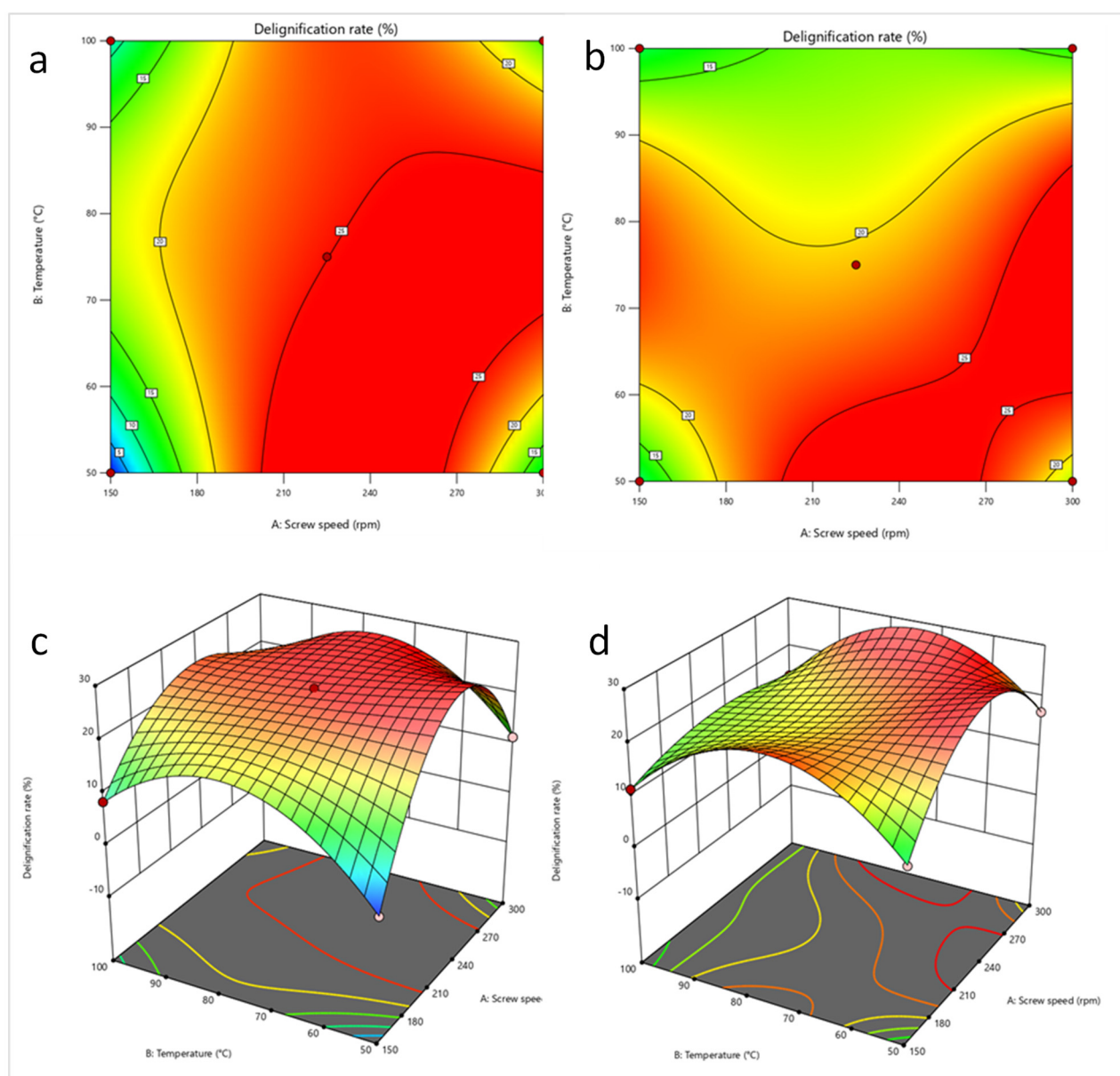


Figure 8. 2D and 3D response surface of the optimum extrusion conditions for black spruce chips ((a,c): 0% NaOH; (b,d): 15% NaOH).

To verify the reliability of the optimization (model validation), the biomasses were extruded under these conditions. The experimental delignification percentage obtained for CS (Y_2) was 27.4%, which is only 0.8% higher than the predicted delignification. The particle size was 204.6 μm , and the specific surface area was 597.9 cm^2/cm^3 . The central composite design for CS improved the delignification percentage by 22%, and the response surface method improved it by 5%. For BS, Y_1 was 22.5% compared to 28.9% (prediction), resulting in a difference of 6.5%. The extrudate took the form of a fine powder (55 μm), with a very high specific surface area (2402 cm^2/cm^3). Under these conditions, the spaces between the particles are very small. It leads to high electrostatic and van der Waals forces and limits good mixing between the extrudate and the sulfuric acid during the Klason lignin analysis, resulting in the formation of agglomerated particles [43]. This explains the lower delignification percentage obtained (more than 5%). Nevertheless, both optimizations were successful as the delignification percentages obtained from both optimization models are significantly higher than without their use. Additionally, they involved very low

temperatures (50 °C and 65 °C instead of 190 °C), while no chemicals were necessary, and the screw rotation speed was low to achieve stable extrusion conditions.

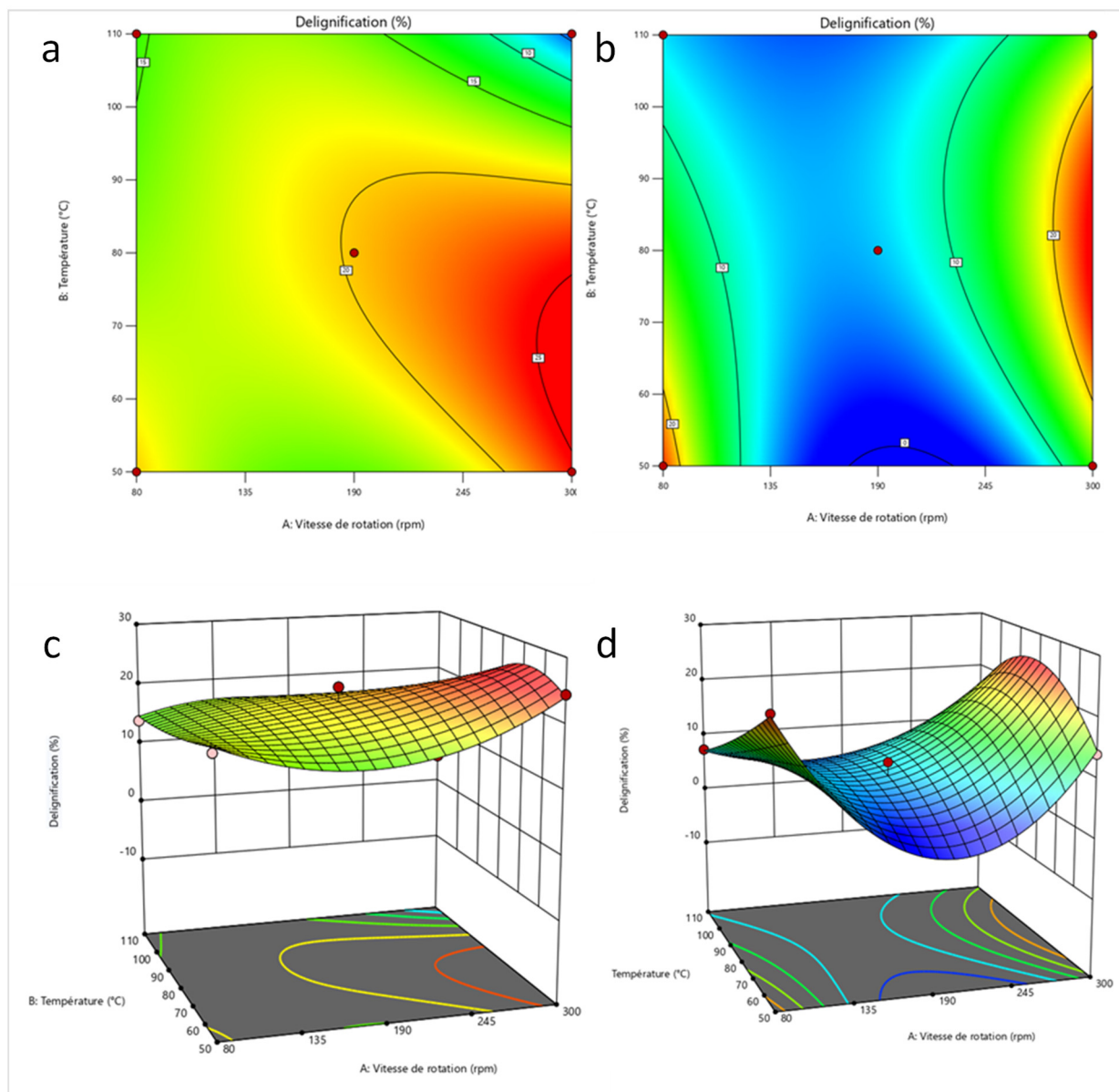


Figure 9. 2D and 3D response surface of the optimum extrusion conditions for corn stover ((a,c): 0% NaOH; (b,d): 15% NaOH).

Table 7. Optimization constraints of the models.

Criteria	Unit	Limit	Goal	Relative Importance (1 to 5)
Particle size	mm	1–1.5	Minimize	+++ (3)
Screw rotation speed	rpm	190–300	Minimize	+ (1)
NaOH concentration	w/w	0–15	Minimize	++ (2)
Temperature	°C	50–90	Minimize	+ (1)
Delignification	% (w/w)	>20	Maximize	+++++ (5)

+ corresponds to the lowest importance, ++ corresponds to moderate-low importance, +++ corresponds to medium importance and +++++ corresponds to the highest importance.

3.7. Effect of Extrusion on the Biomass Structure

Scanning electron microscopy (SEM) images before and after treatment were used to visualize the effect of extrusion on the structural organization of the processed biomass (Figure 10). Images of the raw biomasses show a compact and ordered structure, with larger parts and small fragments of residues. Macrofibers are organized side by side. In some places, the pieces are crumbling, with peels (small plates) more or less detached from the rest of the structure. These peelings are the result of the milling blades used to reduce the particle sizes from 2–5 mm to 1 mm. In contrast, the images of the extruded biomasses present a different morphology. Extrusion has a defibrillation effect on the biomass. The microfibers in the extrudates are shortened and detached from each other. They are twisted, interlocked, and chaotically disorganized. Their appearance is much rougher and more irregular than the raw biomass. Nodules can be observed, which are actually microfibers agglomerated under the action of shear forces (kneading screw elements). The extrudates also become a micropore-filled structure, with the micropores being created by the spaces left between the macro- and microfibers. The result is a significant increase of the specific surface area of the BSE and CSE. These observations were confirmed by analyzing the specific surface areas of the extrudates. Raw CS (ground to 0.5 mm) and BS (ground to 0.5 mm) had specific surface areas of $398.9 \text{ cm}^2/\text{cm}^3$ and $511.5 \text{ cm}^2/\text{cm}^3$, respectively. On the other hand, their respective optimized extrudates had $1183.3 \text{ cm}^2/\text{cm}^3$ and $1569.1 \text{ cm}^2/\text{cm}^3$, respectively. This represents a four-times increase in the specific surface area over the raw residues. According to Mosier et al. [44], the disruption of the ordered structure of the raw biomass increases the specific surface area accessible to the enzymes in the microfibers, thus enhancing the enzymatic digestibility. Furthermore, extrusion does not change the elemental composition of the biomass in terms of carbon, hydrogen, nitrogen, and sulfur. The CHNS analysis of the optimized BSE and CSE gave the same relative proportion compared to their respective raw biomass. However, comparing the FTIR spectra of the raw biomasses and their optimized extrudates, it was clear that extrusion significantly changed the molecular organization of BS, but not so much for CS (Figure 11). The spectra show the absorption of infrared radiation by the biomass samples, with peaks corresponding to the vibrational frequencies of different functional groups. In the raw biomasses, the functional groups are ordered and engaged in several types of bonds. They have less freedom to vibrate or stretch, consequently displaying lower absorbance. For BSE, the peaks are clearly marked and distinguishable from one another. This indicates that the extrusion processing was able to de-structure the lignocellulose complex by efficiently breaking multiple bonds. Several key functional groups were affected (Table 8), but the most important were those at 1024 , 2897 , and 3335 cm^{-1} attributed respectively to C-O stretching in hemicellulose, H-C-H stretching in cellulose, and phenols ring vibration in lignin [45–48]. The 2358 cm^{-1} peak is present in the extrudates but absent from the spectra of the raw biomasses. This peak corresponds to carbon dioxide (CO_2) which might be formed from the thermal degradation (oxidation/combustion) of the biomass in the extruder, although the optimum extrusions were performed at low temperatures: 50°C for BS and 65°C for CS. This information confirms the hypothesis that higher temperatures can occur locally within the biomass during the extrusion step due to high shear forces (friction) in the confined space between the screws and the barrel.

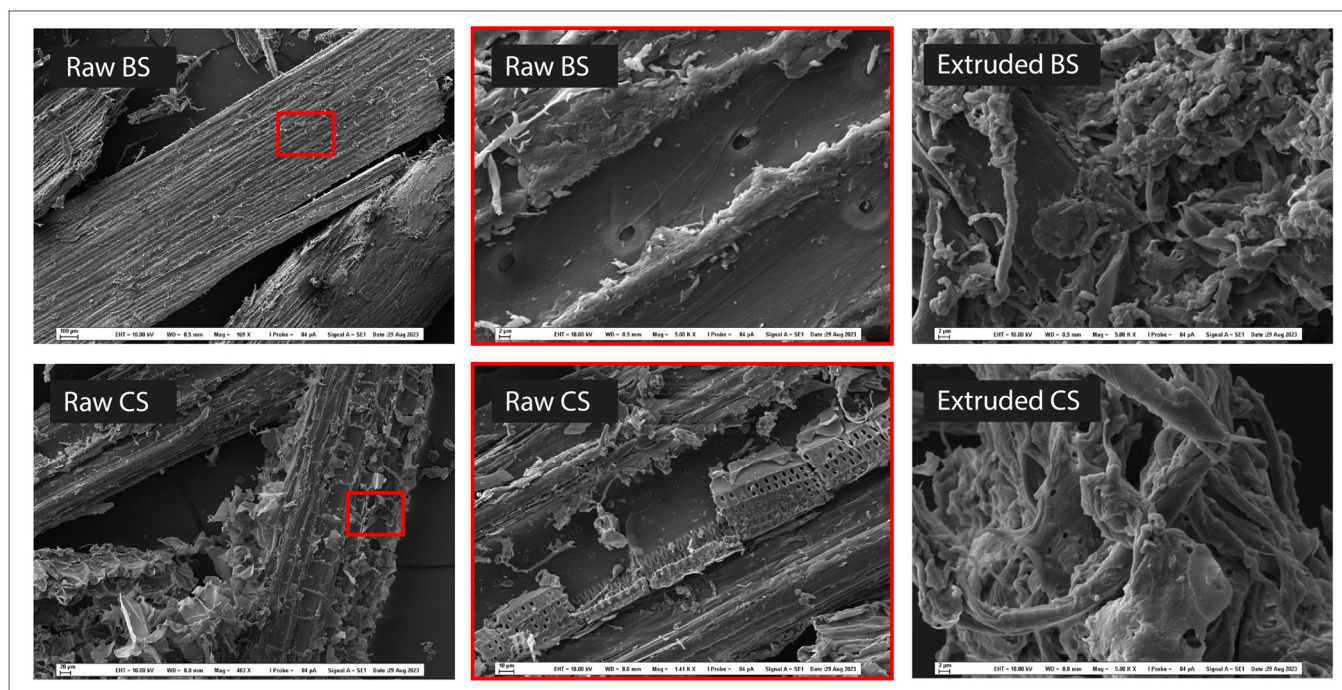


Figure 10. Scanning electron microscope images of black spruce chips (BS) and corn stover (CS) before and after extrusion.

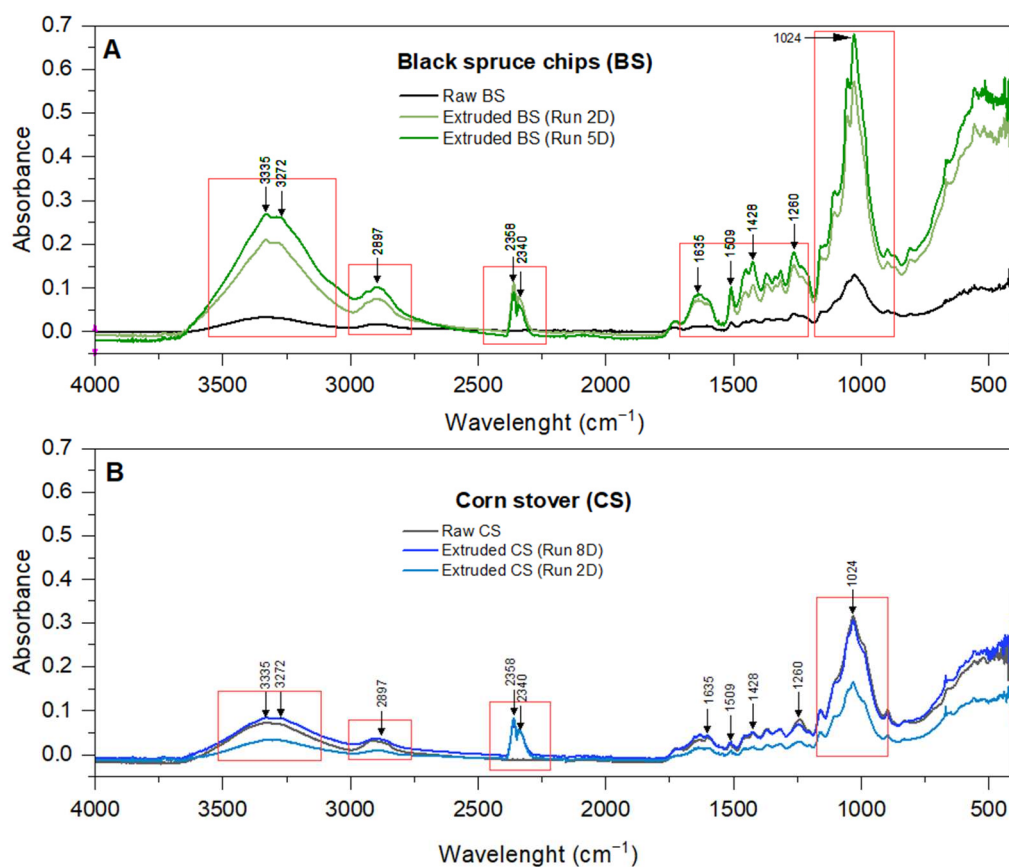


Figure 11. FTIR spectra of black spruce chips (A) and corn stover (B) before and after extrusion.

GC/MS analysis of BSE and CSE was performed to detect the formation of non-desirable compounds in the extrudates, especially furfural and 5-hydroxymethylfurfural (HMF). No furfural and HMF were detected in both biomasses (See Appendices A and B).

Furfural and HMF are pentoses (C5) and hexose (C6) derivatives usually generated from the dehydration of furan and pyran rings. Xylose, the main hemicellulose component, is the main source of furfural, while glucose, the monomer of cellulose, is the main source of HMF. Furfural and HMF usually appear under harsh chemical or thermal pretreatment conditions and are inhibitors of enzymatic activity [49]. Although furfural and HMF have an important market value, when the pretreatment is related to bioethanol production [50,51], their formation is not desired. Chemical and hydrothermal pretreatments, such as ionic liquid, deep eutectic solvent, steam explosion, and liquid hot water, are generally confronted with the problem of inhibitor formation [52–54]. Acetic acid was detected in CSE. Although acetic acid has limited inhibitory effect on the activity of cellulases [54,55], depending on the concentration, it may affect the yeast's enzymatic activity during ethanol production [54]. For example, while investigating the effect of acetic acid on the growth of a strain of the most used ethanol-production yeast (*Saccharomyces cerevisiae*), Narendranath et al. [56] reported a minimum inhibitory concentration (MIC) of 0.6% *w/v* (100 mM) for acetic acid to affect the development of the yeast. Inhibitor formation is one of the primary concerns of lignocellulosic biomass pretreatment for second-generation bioethanol production. Many studies investigated and proposed innovative approaches to remove such compounds or to improve the ethanol yield. Kumar et al. [57] presented an interesting overview of strategies and trending methods for inhibitors removal including biological methods, such as microbial electrochemical cells and recombinant *Escherichia coli*. Wimalascena et al. [58], looking for an inhibitor-tolerant ethanol yeast strain. They screened 90 strains of *Saccharomyces* spp. and found *S. cerevisiae* strain, YPS 606, as a general tolerant strain to inhibitors. The ethanolic fermentation with *S. cerevisiae* strain, YPS 606, was not affected by the presence of inhibitors (10 mM acetic acid, 5 mM formic acid, 5 mM levulinic acid, 5 mM HMF, 5 mM furfural and 5 mM vanillin in combination). As for Khan et al. [59], they proposed a different approach for ethanol yield enhancement: the dewaxing of the biomass before the pretreatment, combined with a post-pretreatment washing. This technique was used successfully with acid (sulfuric acid, 2.95 wt.%) and alkaline (sodium hydroxide, 2.17 M) pretreatments to convert tobacco residues into bioethanol. The sugar yield was improved by more than 23% when the biomass was dewaxed before the pretreatments compared to pretreatments without the dewaxing step. As for the ethanol production, the dewaxed alkali pretreated biomass improved the yield by 34% compared to the undewaxed alkali biomass. The drawback of this method is however the additional steps, energy and water consumption associated to this approach. To be viable, the economic profitability of the ethanol yield enhancement must outweigh the drawbacks.

Table 8. Functional groups detected in the biomass samples by FTIR spectroscopy: adapted from [45–48].

Wavelength (cm ^{−1})	Functional Group
838	Aromatic C-H out-of-plane bending vibration
896	C-O, C=C, and C-C-O in hemicellulose
1024	C-O stretching in hemicellulose, C=C, C-C-O vibrational stretching
1260	C-O of guaiacyl rings in lignin
1428	Aromatic C-C stretching, deformation of C-H, CH ₂ scissoring in cellulose
1509	Aromatic skeletal vibration
1635	C=O stretching in lignin
2340–2358	CO ₂ stretching
2897	Alkanes/primary amines or alkanes and acids/aliphatic H-C-H stretching cellulose

3.8. Energy Consumption and Pretreatment Cost

Energy consumption and the associated costs of biomass pretreatment are of significant importance for large-scale (commercial/industrial) production. Some pretreatments having high enzymatic hydrolysis rates are not suitable for industrial use due to their high costs. This is especially true for chemical pretreatments such as Organosolv, ionic liquid, and ozonolysis, where the cost of the chemicals remains high [60]. In terms of mechanical pretreatment, the main challenge is energy consumption. One of the advantages of extrusion technology is its low electrical energy consumption. The mini-extruder (11 mm) used in this study had specifications of 16 A and 230 V. Under the optimized conditions of this study, the pretreatment flow rate was 1.5 g/min of biomass, resulting in an energy consumption of 40 kWh/kg of biomass. To this consumption must be added the biomass grinding step to reduce the chips or stover size to 1 mm before extrusion. The electrical specifications of the cutting mill (Pulverisette 15) used in this study were: 100–120 V/1~, 60 Hz, 1900 W, 3 Nm with 2.1 kW (drive). It took about 45 min to grind 1 kg of black spruce from 2–5 mm to 1 mm, and about 25 min to grind 1 kg of corn stover from 2–5 mm to 1 mm. The energy consumption was 1.43 kWh/kg of ground black spruce and 0.8 kWh of ground corn stover. In the province of Quebec (Canada), the energy consumption cost is 6.704 ¢/kWh for the first 40 kWh of the day and 10.342 ¢/kWh for each kWh after. Pretreating 1 kg of black spruce with the 11 mm mini-extruder would theoretically cost 1.97 \$ USD (2.83 \$ CAD), while pretreating 1 kg of corn stover would cost 1.92 \$ USD (2.76 \$ CAD) [61]. Energy savings could be even better with larger extruders able to process several tons of biomass. For example, Hjorth et al. [62] used a large twin-screw extruder (Model MSZ B55e; Lehmann Maschinenbau GmbH, Pöhl, Germany) with an energy consumption of only 4 to 10 kWh/ton of biomass. Additionally, they included 150 kWh/ton of biomass for heating the extruder from 20 °C to 150 °C, resulting in a total consumption of 160 kWh/ton of biomass to start the extrusion, and similar values when the desired temperature is reached. By optimizing the extrusion process using a design of experiment, the extrusion temperature can be significantly reduced, as reported in this study for BS (50 °C) and CS (65 °C). Nevertheless, calculations must be done for each specific equipment, biomass, and conditions.

3.9. Perspective for Future Work

The results discussed above highlighted important facts about BS and CS extrusion. They showed that extrudates with very small particle sizes and large specific surface areas can be obtained from raw CS and BS larger than 1 mm in size. This is achieved through the strong effect of the extruder screws on the morphology of the biomasses, which is highly desirable for enzymatic activity (larger specific surface area). Additionally, over 20% delignification was achieved without the use of chemicals (NaOH) and low extrusion temperatures. These conditions suggested that the energy consumption for extrusion and heating can be significantly reduced on a larger scale. Furthermore, extrusion is a technology generating no enzyme inhibitors such as furfural or 5-hydroxymethylfurfural, as confirmed by GC/MS analyses. Extrusion does not require post-washing operations prior to enzymatic hydrolysis for the recovery of sugars (glucose, xylose, etc.) [63]. Considering the elemental composition of the biomasses studied, they both have high carbon content (47.6% for BS and 43.9% for CS), and CS as a high C/N (carbon/nitrogen) ratio of 81:1. These elemental compositions were not changed by the extrusion process. All these characteristics make BSE and CSE excellent candidates for biodelignification by white rot fungi (WRF). White rot fungi can effectively delignify lignocellulosic biomasses under favorable conditions, including a nitrogen/carbon ratio of 50:1–122:1, temperature range of 25–40 °C, particle size range of mm to µm, large specific surface area, agitation, pH range of 4–9, and low

water activity [64–66]. The biodelignification is achieved through an enzyme system mainly consisting of three ligninolytic enzymes: lignin peroxidase, manganese peroxidase, and laccase, which are known to break carbon-carbon bonds to mineralize lignin. Depending on the strain and enzyme system, part of the holocellulose (cellulose and hemicellulose) may be consumed during fermentation [67]. However, the recovery of the enzymes produced, and the efficiency of the pretreatment would offset the loss of this portion. Solid-state fermentation is known for its energy efficiency and strategic advantages, such as low volume and water usage, lower contamination risk, concentration of fermentation products, minimal use of chemicals, and low operating costs [68]. Therefore, the proposed pretreatment involves coupling extrusion and biodelignification technology in solid fermentation with fungal strains. To the best of our knowledge, this approach has never been attempted before. The extrusion process would enable a minimum preliminary delignification of 20% while reducing the rigidity of the carbohydrate-lignin complex structure. This extrusion action would enhance fungal activity during biodelignification to ensure complete biomass delignification. The development of this new pretreatment approach should be conducted in two stages: (i) evaluate delignification percentage in a laboratory model, and (ii) conduct a techno-economic analysis. The extrusion-biodelignification pretreatment approach could be integrated into the production of second-generation biofuels, with the simultaneous production of commercial ligninolytic enzymes (manganese peroxidase, lignin peroxidase and laccase) and the manufacture of biobased composite materials. This is the subject of a forthcoming study.

4. Conclusions

The analysis and optimization of black spruce chips (BS) and corn stover (CS), through an experimental design, increased their delignification percentage from 2.3% to 27.4% and from 1% to 25.3%, respectively. The delignification percentages were reproducible with a low standard deviation of 1.2% maximum. The two mathematical models developed for BS and CS were strong (p -value < 0.0001) to successfully predict the maximum delignification possible with an error margin of 0.8% for CS and less than 3% (theoretically) for BS. The analysis of extrudate characteristics showed that extrusion reduced particle size from 1000 μm to 55 μm for BS and from 1000 μm to 204.6 μm for CS. It multiplied by more than 4 times BS specific surface area (512 to 2402 cm^2/cm^3) and increased CS specific surface area by 200 cm^2/cm^3 (399 to 597 cm^2/cm^3). Extrusion also created desirable roughness on the particles, generated no inhibitor, and was able to profoundly de-structure the lignocellulosic complex. These results led to the proposition of the development of a new approach to lignocellulosic biomass pretreatment. The novel approach involves combining extrusion and biodelignification in solid fermentation. The outcomes expected from the approach are: (i) a low-cost pretreatment, (ii) complete delignification of biomass from the pretreatment stage, (iii) a significant increase in enzymatic digestibility, and (iv) a substantial improvement in the profitability of lignocellulosic biomass valorization.

Supplementary Materials: The following supporting information can be downloaded at: <https://www.mdpi.com/article/10.3390/waste3020012/s1>, Table S1. Parameter screening. Table S2. Responses of the statistical analyses [69–88].

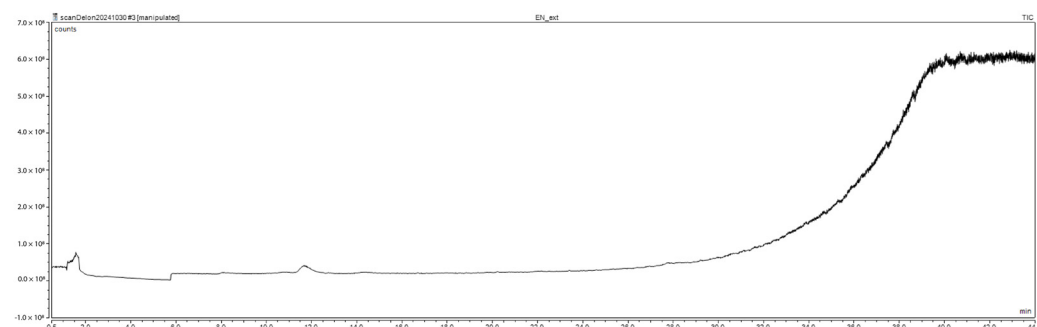
Author Contributions: Conceptualization, Writing—Original Draft: D.K.; Writing—Review & Editing: A.N., E.K., D.R., S.E., M.R. and K.A.; Funding Acquisition, Supervision: K.A. All authors have read and agreed to the published version of the manuscript.

Funding: This work was supported by Institut National de la Recherche Scientifique (INRS) (Grant No. 121486) and the Natural Sciences and Engineering Research Council of Canada (NSERC) (Grant No. RGPIN-2020-05720).

Data Availability Statement: The original contributions presented in this study are included in the article.

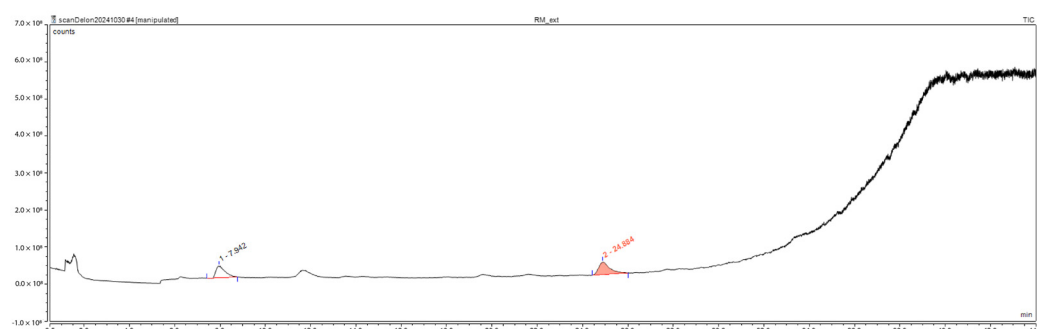
Conflicts of Interest: The authors declare no conflict of interest.

Appendix A. Gas Chromatography/Mass Spectrometry (GC/MS) Results of Black Spruce Extrudate



Peak No.	Ret. Time min	1st Hit SI	Library Compound	Area counts*min	CAS Number
TIC	TIC	TIC	TIC	TIC	TIC
1	-	-	-	-	-

Appendix B. Gas Chromatography/Mass Spectrometry (GC/MS) Results of Corn Stover Extrudate



Peak No.	Ret. Time min	1st Hit SI	Library Compound	Area counts*min	CAS Number
TIC	TIC	TIC	TIC	TIC	TIC
1	7.94	948	Acetic acid	14,845,990.4	64-19-7
2	24.88	738	Benzofuran, 2,3-dihydro-	19,141,586.9	496-16-2

References

1. Ab Rasid, N.S.; Shamjuddin, A.; Abdul, R.A.Z.; Amin, N.A.S. Recent advances in green pre-treatment methods of lignocellulosic biomass for enhanced biofuel production. *J. Clean. Prod.* **2021**, *321*, 129038. [[CrossRef](#)]
2. Chakraborty, P.; Kumar, R.; Chakraborty, S.; Saha, S.; Chattaraj, S.; Roy, S.; Banerjee, A.; Tripathy, S.K.; Kumar Ghosh, A.; Jeon, B.-H. Technological advancements in the pretreatment of lignocellulosic biomass for effective valorization: A review of challenges and prospects. *J. Ind. Eng. Chem.* **2024**, *137*, 29–60. [[CrossRef](#)]

3. Audibert, E.; Floret, J.; Quintero, A.; Martel, F.; Rémond, C.; Paës, G. Determination of trade-offs between 2G bioethanol production yields and pretreatment costs for industrially steam exploded woody biomass. *Appl. Energy* **2025**, *380*, 125028. [\[CrossRef\]](#)
4. Kordala, N.; Walter, M.; Brzozowski, B.; Lewandowska, M. 2G-biofuel ethanol: An overview of crucial operations, advances and limitations. *Biomass Convers. Biorefinery* **2024**, *14*, 2983–3006. [\[CrossRef\]](#)
5. Delmer, D.; Dixon, R.A.; Keegstra, K.; Mohnen, D. The plant cell wall—Dynamic, strong, and adaptable—Is a natural shapeshifter. *Plant Cell* **2024**, *36*, 1257–1311. [\[CrossRef\]](#)
6. Wang, M.; Zhao, J. Are renewable energy policies climate friendly? The role of capacity constraints and market power. *J. Environ. Econ. Manag.* **2018**, *90*, 41–60. [\[CrossRef\]](#)
7. Watson, M.J.; Machado, P.G.; da Silva, A.V.; Saltar, Y.; Ribeiro, C.O.; Nascimento, C.A.O.; Dowling, A.W. Sustainable aviation fuel technologies, costs, emissions, policies, and markets: A critical review. *J. Clean. Prod.* **2024**, *449*, 141472. [\[CrossRef\]](#)
8. Iram, A.; Cekmecelioglu, D.; Demirci, A. Integrating 1G with 2G Bioethanol Production by Using Distillers' Dried Grains with Solubles (DDGS) as the Feedstock for Lignocellulolytic Enzyme Production. *Fermentation* **2022**, *8*, 705. [\[CrossRef\]](#)
9. Stafford, W.H.L.; Lotter, G.A.; von Maltitz, G.P.; Brent, A.C. Biofuels technology development in Southern Africa. *Dev. S. Afr.* **2019**, *36*, 155–174. [\[CrossRef\]](#)
10. Sharma, B.; Larroche, C.; Dussap, C.-G. Comprehensive assessment of 2G bioethanol production. *Bioresour. Technol.* **2020**, *313*, 123630. [\[CrossRef\]](#)
11. Ong, V.Z.; Wu, T.Y. An application of ultrasonication in lignocellulosic biomass valorisation into bio-energy and bio-based products. *Renew. Sustain. Energy Rev.* **2020**, *132*, 109924. [\[CrossRef\]](#)
12. Caporusso, A.; Giuliano, A.; Liuzzi, F.; De Bari, I. Techno-economic analysis of a lignocellulosic biorefinery producing microbial oils by oleaginous yeasts. *Chem. Eng. Trans.* **2022**, *92*, 637–642. [\[CrossRef\]](#)
13. Gallego-García, M.; Moreno, A.D.; Manzanares, P.; Negro, M.J.; Duque, A. Recent advances on physical technologies for the pretreatment of food waste and lignocellulosic residues. *Bioresour. Technol.* **2023**, *369*, 128397. [\[CrossRef\]](#)
14. Guiao, K.S.; Gupta, A.; Tzoganakis, C.; Mekonnen, T.H. Reactive extrusion as a sustainable alternative for the processing and valorization of biomass components. *J. Clean. Prod.* **2022**, *355*, 131840. [\[CrossRef\]](#)
15. Han, S.-Y.; Park, C.-W.; Endo, T.; Febrianto, F.; Kim, N.-H.; Lee, S.-H. Extrusion process to enhance the pretreatment effect of ionic liquid for improving enzymatic hydrolysis of lignocellulosic biomass. *Wood Sci. Technol.* **2020**, *54*, 599–613. [\[CrossRef\]](#)
16. Chevalier, A.; Evon, P.; Monlau, F.; Vandenbossche, V.; Sambusiti, C. Twin-Screw Extrusion Mechanical Pretreatment for Enhancing Biomethane Production from Agro-Industrial, Agricultural and Catch Crop Biomasses. *Waste* **2023**, *1*, 497–514. [\[CrossRef\]](#)
17. Akobi, C.; Yeo, H.; Hafez, H.; Nakhla, G. Single-stage and two-stage anaerobic digestion of extruded lignocellulosic biomass. *Appl. Energy* **2016**, *184*, 548–559. [\[CrossRef\]](#)
18. Shukla, A.; Kumar, D.; Girdhar, M.; Kumar, A.; Goyal, A.; Malik, T.; Mohan, A. Strategies of pretreatment of feedstocks for optimized bioethanol production: Distinct and integrated approaches. *Biotechnol. Biofuels Bioprod.* **2023**, *16*, 44. [\[CrossRef\]](#)
19. Konan, D.; Koffi, E.; Ndao, A.; Peterson, E.C.; Rodrigue, D.; Adjallé, K. An Overview of Extrusion as a Pretreatment Method of Lignocellulosic Biomass. *Energies* **2022**, *15*, 3002. [\[CrossRef\]](#)
20. WSP. *Inventaire de la Biomasse Disponible Pour Produire de la Bioénergie et Portrait de la Production de la Bioénergie sur le Territoire Québécois*; Rapport Réalisé par WSP Canada Inc., pour le Compte du Ministère de l'Énergie et des Ressources Naturelles; Ministère de l'énergie et des Ressources Naturelles: Québec City, QC, Canada, 2021; p. 277.
21. Van Soest, P.v.; Robertson, J.B.; Lewis, B.A. Methods for dietary fiber, neutral detergent fiber, and nonstarch polysaccharides in relation to animal nutrition. *J. Dairy Sci.* **1991**, *74*, 3583–3597. [\[CrossRef\]](#)
22. Sluiter, A.; Hames, B.; Ruiz, R.; Scarlata, C.; Sluiter, J.; Templeton, D.; Crocker, D. Determination of structural carbohydrates and lignin in biomass. *Lab. Anal. Proced.* **2008**, *1617*, 1–16.
23. Konan, D.; Rodrigue, D.; Koffi, E.; Elkoun, S.; Ndao, A.; Adjallé, K. Combination of Technologies for Biomass Pretreatment: A Focus on Extrusion. *Waste Biomass Valorization* **2024**, *15*, 4519–4540. [\[CrossRef\]](#)
24. Sheng, C.; Azevedo, J.L.T. Estimating the higher heating value of biomass fuels from basic analysis data. *Biomass Bioenergy* **2005**, *28*, 499–507. [\[CrossRef\]](#)
25. Liu, K.-X.; Li, H.-Q.; Zhang, J.; Zhang, Z.-G.; Xu, J. The effect of non-structural components and lignin on hemicellulose extraction. *Bioresour. Technol.* **2016**, *214*, 755–760. [\[CrossRef\]](#)
26. Zhang, J.; Wang, Y.-H.; Qu, Y.-S.; Wei, Q.-Y.; Li, H.-Q. Effect of the organizational difference of corn stalk on hemicellulose extraction and enzymatic hydrolysis. *Ind. Crops Prod.* **2018**, *112*, 698–704. [\[CrossRef\]](#)
27. Mustafa, A.F.; Hassanat, F.; Berthiaume, R.R. In situ forestomach and intestinal nutrient digestibilities of sweet corn residues. *Anim. Feed. Sci. Technol.* **2004**, *114*, 287–293. [\[CrossRef\]](#)
28. Zhang, R.; Ma, S.; Li, L.; Zhang, M.; Tian, S.; Wang, D.; Liu, K.; Liu, H.; Zhu, W.; Wang, X. Comprehensive utilization of corn starch processing by-products: A review. *Grain Oil Sci. Technol.* **2021**, *4*, 89–107. [\[CrossRef\]](#)

29. Fang, H.; Deng, J.; Zhang, T. Dilute Acid Pretreatment of Black Spruce Using Continuous Steam Explosion System. *Appl. Biochem. Biotechnol.* **2011**, *163*, 547–557. [CrossRef]
30. Zheng, J.; Choo, K.; Rehmann, L. The effects of screw elements on enzymatic digestibility of corncobs after pretreatment in a twin-screw extruder. *Biomass Bioenergy* **2015**, *74*, 224–232. [CrossRef]
31. Long, J.; Xu, Y.; Wang, T.; Yuan, Z.; Shu, R.; Zhang, Q.; Ma, L. Efficient base-catalyzed decomposition and in situ hydrogenolysis process for lignin depolymerization and char elimination. *Appl. Energy* **2015**, *141*, 70–79. [CrossRef]
32. Velasco, S.; Román, F.L.; White, J.A. On the Clausius–Clapeyron Vapor Pressure Equation. *J. Chem. Educ.* **2009**, *86*, 106. [CrossRef]
33. Gu, B.J.; Dhumal, G.S.; Wolcott, M.P.; Ganjyal, G.M. Disruption of lignocellulosic biomass along the length of the screws with different screw elements in a twin-screw extruder. *Bioresour. Technol.* **2019**, *275*, 266–271. [CrossRef] [PubMed]
34. Chang, Y.H.; Ng, P.K.W. Effects of Extrusion Process Variables on Quality Properties of Wheat-Ginseng Extrudates. *Int. J. Food Prop.* **2011**, *14*, 914–925. [CrossRef]
35. Román-Ramírez, L.A.; Marco, J. Design of experiments applied to lithium-ion batteries: A literature review. *Appl. Energy* **2022**, *320*, 119305. [CrossRef]
36. NIST. Engineering Statistics Handbook. 2024. Available online: <https://www.itl.nist.gov/div898/handbook/pri/pri.htm> (accessed on 31 October 2024).
37. Jung, W.; Savithri, D.; Sharma-Shivappa, R.; Kolar, P. Changes in Lignin Chemistry of Switchgrass due to Delignification by Sodium Hydroxide Pretreatment. *Energies* **2018**, *11*, 376. [CrossRef]
38. Augustina, S.; Wahyudi, I.; Dwianto, W.; Darmawan, T. Effect of Sodium Hydroxide, Succinic Acid and Their Combination on Densified Wood Properties. *Forests* **2022**, *13*, 293. [CrossRef]
39. Yang, J.; Sun, M.; Jiao, L.; Dai, H. Molecular Weight Distribution and Dissolution Behavior of Lignin in Alkaline Solutions. *Polymers* **2021**, *13*, 4166. [CrossRef]
40. Komatsu, T.; Yokoyama, T. Revisiting the condensation reaction of lignin in alkaline pulping with quantitativity part I: The simplest condensation between vanillyl alcohol and creosol under soda cooking conditions. *J. Wood Sci.* **2021**, *67*, 45. [CrossRef]
41. Huang, Y.L.; Ma, Y.S. Optimization of the extrusion process for preparation of soluble dietary fiber-enriched calamondin pomace and its influence on the properties of bread. *J. Food Sci. Technol.* **2019**, *56*, 5444–5453. [CrossRef]
42. Calcio Gaudino, E.; Grillo, G.; Manzoli, M.; Tabasso, S.; Maccagnan, S.; Cravotto, G. Mechanochemical Applications of Reactive Extrusion from Organic Synthesis to Catalytic and Active Materials. *Molecules* **2022**, *27*, 449. [CrossRef]
43. Feng, J.Q.; Hays, D.A. Relative importance of electrostatic forces on powder particles. *Powder Technol.* **2003**, *135–136*, 65–75. [CrossRef]
44. Mosier, N.; Hendrickson, R.; Ho, N.; Sedlak, M.; Ladisch, M.R. Optimization of pH controlled liquid hot water pretreatment of corn stover. *Bioresour. Technol.* **2005**, *96*, 1986–1993. [CrossRef] [PubMed]
45. Goncalves, D.; Orišková, S.; Matos, S.; Machado, H.; Vieira, S.; Bastos, D.; Gaspar, D.; Paiva, R.; Bordado, J.C.; Rodrigues, A.; et al. Thermochemical Liquefaction as a Cleaner and Efficient Route for Valuing Pinewood Residues from Forest Fires. *Molecules* **2021**, *26*, 7156. [CrossRef]
46. Ahmed, A.; Bakar, M.S.A.; Razzaq, A.; Hidayat, S.; Jamil, F.; Amin, M.N.; Sukri, R.S.; Shah, N.S.; Park, Y.-K. Characterization and Thermal Behavior Study of Biomass from Invasive Acacia mangium Species in Brunei Preceding Thermochemical Conversion. *Sustainability* **2021**, *13*, 5249. [CrossRef]
47. Kurian, J.K.; Garipey, Y.; Orsat, V.; Raghavan, G.S.V. Microwave-assisted lime treatment and recovery of lignin from hydrothermally treated sweet sorghum bagasse. *Biofuels* **2015**, *6*, 341–355. [CrossRef]
48. Silvestre, W.P.; Galafassi, P.L.; Ferreira, S.D.; Godinho, M.; Pauletti, G.F.; Baldasso, C. Fodder radish seed cake biochar for soil amendment. *Environ. Sci. Pollut. Res.* **2018**, *25*, 25143–25154. [CrossRef]
49. Koopman, F.; Wierckx, N.; de Winde, J.H.; Ruijsenaars, H.J. Identification and characterization of the furfural and 5-(hydroxymethyl) furfural degradation pathways of *Cupriavidus basilensis* HMF14. *Proc. Natl. Acad. Sci. USA* **2010**, *107*, 4919–4924. [CrossRef]
50. Mittal, A.; Pilath, H.M.; Johnson, D.K. Direct Conversion of Biomass Carbohydrates to Platform Chemicals: 5-Hydroxymethylfurfural (HMF) and Furfural. *Energy Fuels* **2020**, *34*, 3284–3293. [CrossRef]
51. Yong, K.J.; Wu, T.Y.; Lee, C.B.T.L.; Lee, Z.J.; Liu, Q.; Jahim, J.M.; Zhou, Q.; Zhang, L. Furfural production from biomass residues: Current technologies, challenges and future prospects. *Biomass Bioenergy* **2022**, *161*, 106458. [CrossRef]
52. Behera, S.; Arora, R.; Nandhagopal, N.; Kumar, S. Importance of chemical pretreatment for bioconversion of lignocellulosic biomass. *Renew. Sustain. Energy Rev.* **2014**, *36*, 91–106. [CrossRef]
53. Ilanidis, D.; Stagge, S.; Jönsson, L.J.; Martín, C. Hydrothermal Pretreatment of Wheat Straw: Effects of Temperature and Acidity on Byproduct Formation and Inhibition of Enzymatic Hydrolysis and Ethanol Fermentation. *Agronomy* **2021**, *11*, 487. [CrossRef]
54. Ko, J.K.; Um, Y.; Park, Y.-C.; Seo, J.-H.; Kim, K.H. Compounds inhibiting the bioconversion of hydrothermally pretreated lignocellulose. *Appl. Microbiol. Biotechnol.* **2015**, *99*, 4201–4212. [CrossRef] [PubMed]

55. Jing, X.; Zhang, X.; Bao, J. Inhibition Performance of Lignocellulose Degradation Products on Industrial Cellulase Enzymes During Cellulose Hydrolysis. *Appl. Biochem. Biotechnol.* **2009**, *159*, 696–707. [CrossRef]
56. Narendranath, N.V.; Thomas, K.C.; Ingledew, W.M. Effects of acetic acid and lactic acid on the growth of *Saccharomyces cerevisiae* in a minimal medium. *J. Ind. Microbiol. Biotechnol.* **2001**, *26*, 171–177. [CrossRef]
57. Kumar, V.; Yadav, S.K.; Kumar, J.; Ahluwalia, V. A critical review on current strategies and trends employed for removal of inhibitors and toxic materials generated during biomass pretreatment. *Bioresour. Technol.* **2020**, *299*, 122633. [CrossRef]
58. Wimalasena, T.T.; Greetham, D.; Marvin, M.E.; Liti, G.; Chandel, Y.; Hart, A.; Louis, E.J.; Phister, T.G.; Tucker, G.A.; Smart, K.A. Phenotypic characterisation of *Saccharomyces* spp. yeast for tolerance to stresses encountered during fermentation of lignocellulosic residues to produce bioethanol. *Microb. Cell Factories* **2014**, *13*, 47. [CrossRef]
59. Khan, M.A.K.M.A.; Panakkal, E.J.; Sriariyanun, M.; Gundupalli, M.P.; Roddecha, S.; Katam, K.; Jayaprakash, J.; Cheenkachorn, K. Dewaxing and Post-Pretreatment Washing: Impact on Sugar and Ethanol Yields from Tobacco Residue. *Appl. Sci. Eng. Prog.* **2024**, *17*, 7495. [CrossRef]
60. Sidana, A.; Yadav, S.K. Recent developments in lignocellulosic biomass pretreatment with a focus on eco-friendly, non-conventional methods. *J. Clean. Prod.* **2022**, *335*, 130286. [CrossRef]
61. HydroQuébec. 2024 Tarif D'électricité, En Vigeur le 1er Avril 2024; Bibliothèque et Archives Nationales du Québec: Québec, QC, Canada, 2024; pp. 1–220. Available online: <https://www.hydroquebec.com/data/documents-donnees/pdf/tarifs-electricite.pdf?v=20230401> (accessed on 31 October 2024).
62. Hjorth, M.; Gränitz, K.; Adamsen, A.P.S.; Møller, H.B. Extrusion as a pretreatment to increase biogas production. *Bioresour. Technol.* **2011**, *102*, 4989–4994. [CrossRef]
63. Duque, A.; Manzanares, P.; Ballesteros, M. Extrusion as a pretreatment for lignocellulosic biomass: Fundamentals and applications. *Renew. Energy* **2017**, *114*, 1427–1441. [CrossRef]
64. Allen, L.V., Jr. Quality Control: Water Activity Considerations for Beyond-use Dates. *Int. J. Pharm. Compd.* **2018**, *22*, 288–293. [PubMed]
65. Sala, A.; Barrena, R.; Artola, A.; Sánchez, A. Current developments in the production of fungal biological control agents by solid-state fermentation using organic solid waste. *Crit. Rev. Environ. Sci. Technol.* **2019**, *49*, 655–694. [CrossRef]
66. Montoya, S.; Patiño, A.; Sánchez, Ó.J. Production of Lignocellulolytic Enzymes and Biomass of *Trametes versicolor* from Agro-Industrial Residues in a Novel Fixed-Bed Bioreactor with Natural Convection and Forced Aeration at Pilot Scale. *Processes* **2021**, *9*, 397. [CrossRef]
67. Millati, R.; Syamsiah, S.; Niklasson, C.; Cahyanto, M.N.; Ludquist, K.; Taherzadeh, M.J. Biological pretreatment of lignocelluloses with white-rot fungi and its applications: A review. *BioResources* **2011**, *6*, 5224–5259. [CrossRef]
68. Machado de Castro, A.; Fragoso dos Santos, A.; Kachrimanidou, V.; Koutinas, A.A.; Freire, D.M.G. Chapter 10—Solid-State Fermentation for the Production of Proteases and Amylases and Their Application in Nutrient Medium Production. In *Current Developments in Biotechnology and Bioengineering*; Pandey, A., Larroche, C., Soccol, C.R., Eds.; Elsevier: Amsterdam, The Netherlands, 2018; pp. 185–210. [CrossRef]
69. Senturk-Ozer, S.; Gevgilili, H.; Kalyon, D.M. Biomass pretreatment strategies via control of rheological behavior of biomass suspensions and reactive twin screw extrusion processing. *Bioresour. Technol.* **2011**, *102*, 9068–9075. [CrossRef]
70. Kelly, A.L.; Brown, E.C.; Coates, P.D. The effect of screw geometry on melt temperature profile in single screw extrusion. *Polym. Eng. Sci.* **2006**, *46*, 1706–1714. [CrossRef]
71. Gatt, E.; Rigal, L.; Vandenbossche, V. Biomass pretreatment with reactive extrusion using enzymes: A review. *Ind. Crops Prod.* **2018**, *122*, 329–339. [CrossRef]
72. Shah, A.; Gupta, M. Comparison of the flow in co-rotating and counter-rotating twinscrew extruders. *ANTEC* **2004**, *1*, 443–447.
73. Vandenbossche, V.; Brault, J.; Vilarem, G.; Hernández-Meléndez, O.; Vivaldo-Lima, E.; Hernández-Luna, M.; Barzana, E.; Duque, A.; Manzanares, P.; Ballesteros, M.; et al. A new lignocellulosic biomass deconstruction process combining thermo-mechano chemical action and bio-catalytic enzymatic hydrolysis in a twin-screw extruder. *Ind. Crops Prod.* **2014**, *55*, 258–266. [CrossRef]
74. Liu, C.; Van Der Heide, E.; Wang, H.; Li, B.; Yu, G.; Mu, X. Alkaline twin-screw extrusion pretreatment for fermentable sugar production. *Biotechnol. Biofuels* **2013**, *6*, 97. [CrossRef]
75. Zheng, J.; Choo, K.; Rehmann, L. Xylose removal from lignocellulosic biomass via a twin-screw extruder: The effects of screw configurations and operating conditions. *Biomass Bioenergy* **2016**, *88*, 10–16. [CrossRef]
76. Duque, A.; Manzanares, P.; Ballesteros, I.; Negro, M.J.; Oliva, J.M.; Gonzalez, A.; Ballesteros, M. Sugar production from barley straw biomass pretreated by combined alkali and enzymatic extrusion. *Bioresour. Technol.* **2014**, *158*, 262–268. [CrossRef] [PubMed]
77. Wahid, R.; Hjorth, M.; Kristensen, S.; Møller, H.B. Extrusion as Pretreatment for Boosting Methane Production: Effect of Screw Configurations. *Energy Fuels* **2015**, *29*, 4030–4037. [CrossRef]
78. Negro, M.J.; Duque, A.; Manzanares, P.; Sáez, F.; Oliva, J.M.; Ballesteros, I.; Ballesteros, M. Alkaline twin-screw extrusion fractionation of olive-tree pruning biomass. *Ind. Crops Prod.* **2015**, *74*, 336–341. [CrossRef]

79. Kuster Moro, M.; Sposina Sobral Teixeira, R.; Sant'Ana da Silva, A.; Duarte Fujimoto, M.; Albuquerque Melo, P.; Resende Secchi, A.; Pinto da Silva Bon, E. Continuous pretreatment of sugarcane biomass using a twin-screw extruder. *Ind. Crops Prod.* **2017**, *97*, 509–517. [[CrossRef](#)]
80. Merci, A.; Urbano, A.; Grossmann, M.V.E.; Tischer, C.A.; Mali, S. Properties of microcrystalline cellulose extracted from soybean hulls by reactive extrusion. *Food Res. Int.* **2015**, *73*, 38–43. [[CrossRef](#)]
81. Karunanithy, C.; Muthukumarappan, K.; Gibbons, W.R. Extrusion pretreatment of pine wood chips. *Appl. Biochem. Biotechnol.* **2012**, *167*, 81–99. [[CrossRef](#)]
82. Karunanithy, C.; Muthukumarappan, K. Optimization of switchgrass and extruder parameters for enzymatic hydrolysis using response surface methodology. *Ind. Crops Prod.* **2011**, *33*, 188–199. [[CrossRef](#)]
83. Kim, S.K.; Park, P.J.; Kim, J.B.; Shahidi, F. Purification and characterization of a collagenolytic protease from the filefish, *Novoden modestrus*. *J. Biochem. Mol. Biol.* **2002**, *35*, 165–171. [[CrossRef](#)]
84. Chundawat, S.P.; Venkatesh, B.; Dale, B.E. Effect of particle size based separation of milled corn stover on AFEX pretreatment and enzymatic digestibility. *Biotechnol. Bioeng.* **2007**, *96*, 219–231. [[CrossRef](#)]
85. Yang, C.; Shen, Z.; Yu, G.; Wang, J. Effect and aftereffect of gamma radiation pretreatment on enzymatic hydrolysis of wheat straw. *Bioresour. Technol.* **2008**, *99*, 6240–6245. [[CrossRef](#)] [[PubMed](#)]
86. Choi, C.H.; Oh, K.K. Application of a continuous twin screw-driven process for dilute acid pretreatment of rape straw. *Bioresour. Technol.* **2012**, *110*, 349–354. [[CrossRef](#)] [[PubMed](#)]
87. Montiel, C.; Hernández-Meléndez, O.; Vivaldo-Lima, E.; Hernández-Luna, M.; Bárzana, E. Enhanced Bioethanol Production from Blue Agave Bagasse in a Combined Extrusion–Saccharification Process. *BioEnergy Res.* **2016**, *9*, 1005–1014. [[CrossRef](#)]
88. Zhang, S.; Keshwani, D.R.; Xu, Y.; Hanna, M.A. Alkali combined extrusion pretreatment of corn stover to enhance enzyme saccharification. *Ind. Crops Prod.* **2012**, *37*, 352–357. [[CrossRef](#)]

Disclaimer/Publisher's Note: The statements, opinions and data contained in all publications are solely those of the individual author(s) and contributor(s) and not of MDPI and/or the editor(s). MDPI and/or the editor(s) disclaim responsibility for any injury to people or property resulting from any ideas, methods, instructions or products referred to in the content.